

Recent advances in electrophoretic deposition of thin-film electrolytes for intermediate-temperature solid oxide fuel cells

Elena Pikalova^{a*}, Elena Kalinina^{bc}, Nadezhda Pikalova^d

Solid oxide fuel cells (SOFCs) have been attracting considerable attention as ecologically friendly and highly efficient power sources with a variety of applications. Modern directions in the SOFCs technology are related to lowering the SOFC operating temperature that require both advanced materials design and development of versatile technologies to fabricate SOFC with thin-film electrolyte membrane to decrease ohmic losses at decreased temperatures. Electrophoretic deposition (EDP) is one of the most technologically flexible and cost-effective methods for the thin film formation currently available. This review highlights challenges and approaches presented in literature to the formation dense thin films based on oxygen-conducting and proton conducting electrolytes, as well as multilayer and composite electrolyte membranes.

keywords: Solid Oxide Fuel Cell, electrophoretic deposition, thin film, solid electrolyte, bilayer membrane, composite electrolyte

© 2023, the Authors. This article is published in open access under the terms and conditions of the Creative Commons Attribution (CC BY) license <http://creativecommons.org/licenses/by/4.0/>.

1. Introduction

Solid Oxide Fuel Cells (SOFCs) as electrochemical energy devices directly converting chemical energy of fuels into electricity have been attracted many efforts for their commercialization due to extraordinary power efficiency, fuel flexibility and environmental friendliness [1]. The established modern trend in the SOFC technology to decreasing the operating temperature to the intermediate temperature (IT) range of 600–750 °C is a reliable way to reduce their production cost using cheaper materials for balance-of-plant components, metal interconnects, electrodes [2–4], and extend the service life of the SOFC-based energy systems [5, 6]. However, the operation at reduced temperatures slowdowns all thermo-activated processes in SOFCs [7]. The main obstacle standing in the way of the realization of the reduced-

temperature approach is a high ohmic resistance of the supporting electrolyte membrane. Thus, Ytria-stabilized Zirconia (YSZ) electrolyte traditionally used in high-temperature SOFCs was replaced by new materials possessing superior conductivity in IT range: oxygen-ion conducting electrolytes based on Scandia-stabilized Zirconia (SSZ) [8], Sr, Mg-doped Lanthanum Gallate (LSGM) [9, 10], doped Ceria [11–13], as well as highly-effective proton conducting electrolytes, particularly, based on Barium cerates/zirconates $\text{BaCe}(\text{Zr})\text{O}_3$ [14–16]. Another effective way to reduce ohmic resistance of a solid-state electrolyte is to reduce its thickness. In this regard, SOFCs with a thin-film electrolyte have been attracting growing research activity [17–19]. State-of-the-art fabrication techniques applicable for manufacturing thin film electrolytes and features of the relative SOFC design (configurations and geometries) were recently overviewed by Dunyushkina [20]. It was shown that using advanced ceramic powder-based technologies and vacuum methods for deposition of thin-film electrolyte layers allowed excellent electrochemical characteristics and

a: Institute of High Temperature Electrochemistry, UB RAS, Yekaterinburg 620066, Russia

b: Institute of Electrophysics, UB RAS, Yekaterinburg 620016, Russia

c: Institute of Natural Sciences and Mathematics, Ural Federal University, Yekaterinburg 620009, Russia

d: Institute of Metallurgy, UB RAS, Yekaterinburg 620016, Russia

* Corresponding author: e.pikalova@list.ru

enhanced power output to be obtained for both metal-supported and planar anode-supported SOFCs.

The method of electrophoretic deposition (EPD) has been developed as one of the cost-effective ceramic methods for forming film coatings on substrates of various shapes and porosity. Fundamentals of the EPD method were presented in detail in the review papers of Besra&Liu [21] and Corni et al. [22]. In the field of SOFC, the application of the EPD method, including the deposition of nanomaterials, was considered in a review by Lee et al. [23]. The features of the preparation of stable suspensions used for EPD of SOFC functional layers were considered in a short review by Aznam et al. [24].

In our recent reviews, we analyzed the basic work on the mechanisms and key factors of EPD, described various theoretical models of deposit growth and coating formation both on dense substrates and in porous structures, and also reported the results of studies on the application of EPD technology for the formation of different SOFC functional layers (electrolytes, electrodes, protective layers for interconnectors including works from 2000 up to 2019 year [25, 26]. The studies on formation of thin-film electrolytes using sputtering and ceramic technologies with focus attention given to the place of EPD among other methods, as well as the work of our scientific group on EPD of electrolyte films on conducting cathode substrates were represented in [27]. Opportunities, challenges and prospects of electrodeposition technology were considered in a review [28], covered electrolytic and electrophoretic deposition, as well as their combined use in the formation of SOFC layers.

The present review contains up-to-date information on the application of the EPD method in SOFC technology, including basic works on deposition principles, preparation of stable suspensions and formation dense electrolyte films. It also summarizes the results obtained by scientific groups on EPD of electrolyte layers based on oxygen-ion and proton-conducting electrolytes. A critical analysis of the current state of work in this area is aimed at identifying key problems and existing opportunities for further development of the EPD method in SOFC technology for the subsequent successful implementation of the solutions found in practice. The review is supposed to be useful for both beginners and experienced researchers involved in the developments of thin-film technologies for SOFC and other electrochemical devices.

2. General principles of electrophoretic deposition

2.1. Electrokinetic phenomena in suspensions

Electrophoretic deposition is a kind of ceramic powder coating technologies, which is based on electrokinetic processes of particle movement in a liquid medium. Schematic representation of the EPD cell is given in Figure 1. Under the influence of an external electric field, the charged particles dispersed in a liquid medium move towards the electrode and deposit.

The excess charge on the particles occurs due to the following processes: adsorption of ions from the dispersion medium onto the particle surface; surface dissociation of ions from the powder particles into the liquid medium; electron transfer between the particles and the liquid medium [30]. The spatial charge separation that arises around the particles in a liquid medium, results in the formation of an electric double layer (EDL), which, in turn, causes electrokinetic phenomena, in particular, electrophoresis.

An electric double layer consists of three parts: surface charge, comprising charged ions (commonly negative) adsorbed on the particle surface; stern layer, containing counterions (charged opposite to the surface charge), immobilized due to the strong influence of the electrostatic force near the particle surface and diffuse layer – a film of the surrounding dispersion medium adjacent to the particle, which contains both free ions and counterions. The most important suspension characteristic is the zeta potential (ζ , mV), which the excess electric charge on the particles and characterizes the stability of the colloidal suspension. When a colloidal

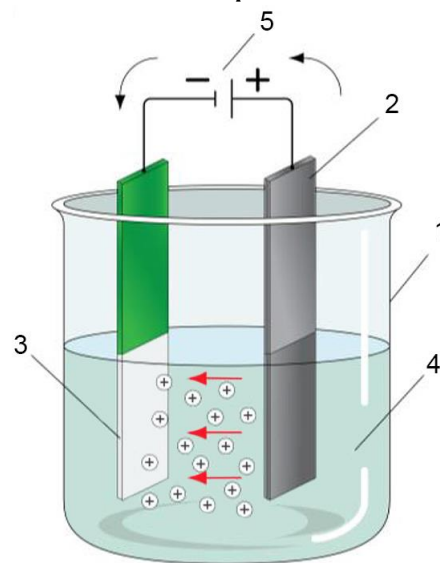


Figure 1 Schematic diagram of an installation for electrophoretic deposition: 1 – reactor, 2 – counter electrode, 3 – porous anode substrate based on NiO-YSZ, 4 – suspension, 5 – electric current source [29].

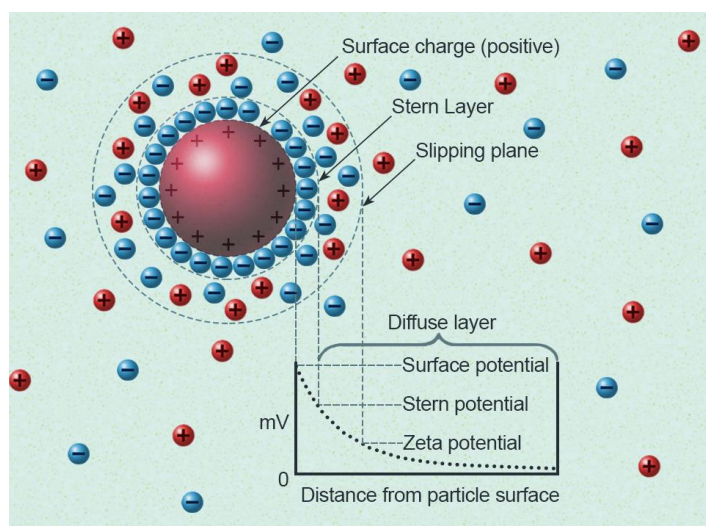


Figure 2 Schematic representation of Ionic distribution in a dispersion medium and potential difference as a function of distance from the charged particle surface.

particle moves in the dispersion medium, a layer of the surrounding liquid remains attached to the particle. Zeta potential corresponds to an electrokinetic potential generated in a slipping plane, where displacement of the liquid medium occurs relative to the layer strongly bounded with the particle (Figure 2).

In terms of the electrophoresis, the zeta potential of particles in the suspension is linearly related to their electrophoretic mobility according to the Henry equation [31]. In turn, the zeta potential increasing corresponds to the electrophoretic mobility and the deposition rate increasing according to the Hamaker equation [32].

The zeta potential value is influenced by ionic composition of a suspension, pH, temperature, and suspension concentration [33–35]. It is interesting to note that interparticle interactions play an important role in nanoparticle suspensions, since they cause the zeta potential decreasing with the increasing suspension concentration [36, 37], which makes it difficult to obtain concentrated nanosuspensions. The methods for the zeta potential measurement were reviewed in [25, 26].

2.2. Stability issues for the suspensions of electrolyte powders

Successful implementation of EPD process requires preparation of stable suspensions [26]. Sedimentation stability in suspensions is characterized by the Stokes law, according to which the sedimentation rate is directly proportional to the square of the particle radius, the difference between the densities of the dispersed phase and the dispersion medium, and inversely proportional to the viscosity of the dispersion medium [33]. The stability of a suspension is the ability to keep the degree of dispersion unchanged over time, i.e. particle sizes and

their individuality. To prevent agglomeration, high particle charge is required to create high electrostatic repulsion between the dispersed particles. However, if repulsive forces between the particles are too strong, the electric field will not be able to overcome these forces and move the particles towards the electrode, thus there will be no deposition. Typically, to stabilize a suspension and ensure stable deposition, a zeta potential value of approximately ± 20 – 30 mV is required [38, 39].

To prepare suspensions, the following treatment methods are used: ultrasonic treatment (UST) and mechanical dispersion [40, 41], treatment in a dissolver [42], stirring in a magnetic stirrer [43], as well as a combination of UST and centrifugation methods [44]. Suspensions of microsized powders are characterized by better aggregative stability, i.e. preservation of the dispersed composition, in comparison with the suspensions of nanoparticles, even the latter being ultrasonically treated. Not only single particles are formed in the process of the preparation of the suspensions based on nanosized powders, but also a significant proportion of their aggregates, which can be destroyed by a long-term ultrasonic treatment (exceeding 2 hours, with organization of the simultaneous suspension cooling) and also separated from the suspension by centrifugation [44]. Any significant changes in the dispersed composition during UST are not representative of aggregatively stable suspensions of microsized powders [45], while for the suspensions based on nanosized powders they may be very pronounced [44, 46–48].

The selection of the appropriate dispersing medium plays an important role in ensuring both aggregative and sedimentation stability of the suspension. Dispersion media affect the stability of the suspension due to different solvating abilities [49, 50]. Non-aqueous media based on alcohols, ketones, such as acetylacetone or their mixtures are most commonly used for the preparation of the suspensions of electrolyte powders (Table 1). The use of an aqueous medium is not typical for creating gas-tight electrolyte films, since EPD from an aqueous suspension is accompanied by electrolysis and the release of bubbles. The formed gas bubbles can be incorporated in the deposit and yield coatings with closed porosity.

The quality of YSZ films obtained by aqueous EPD was improved by pulses or alternate currents/voltages instead of direct current implementation [52, 87, 89].

Interesting to note, that the water, presented as an impurity in alcohols, can be a source of hydrogen ions, which provide better electrical conductivity of the suspension for EPD, thus increasing the deposition rate. The optimal amount of the water impurity in non-aqueous suspensions was found to be in a range of

Table 1 – Dispersion media used for the preparation of suspensions based on various solid-state electrolyte powders.

Dispersion medium	Electrolyte	Refs
Alcohols (ethanol, isopropanol, l-propanol, n- propanol, n- butanol)	YSZ	[49], [51], [52], [53], [54], [55], [56], [57], [58]
	SSZ	[59]
	doped CeO ₂	[50], [53], [60], [61], [62]
	LSGM	[53]
	LSO ^a	[63], [64]
Ketones (acetone, acetylacetone)	BaCe(Zr)YO ₃	[65], [66]
	YSZ	[56], [57], [67], [68], [69], [70]
	SSZ	[71]
Mixed alcohol/ketone medium	doped CeO ₂	[50], [72], [73],
	BaCe(Zr)YO ₃	[65], [74], [75]
	YSZ	[29], [44], [56], [76], [77],
	doped CeO ₂	[47], [50], [78], [79], [80]
Distilled water	LSGM	[41]
	BaCe(Zr)YO ₃	[45], [81], [82], [83], [84]
	YSZ	[85], [86]
	doped CeO ₂	[87], [88]

^a – lanthanum silicate oxyapatite.

2–4 vol. % [90, 91]. It should be noted that the formation of bubbles in coatings is possible with the use of a non-aqueous suspensions in the EPD of oxide ceramics with the presence of a fraction of the metal component in the nanosized powder composition [92].

The concentration of protons in a suspension (pH) greatly affects the zeta potential, in particular, in non-aqueous suspensions [78], since protons are adsorbed on the particles surface and become potential-determining ions. The pH value in the suspension can be adjusted by adding hydrochloric acid [93, 94], or carboxylic acids [95, 96], and various bases – triethanolamine (TEA), monoethanolamine (MEA), and 6-amino-1-hexanol (AH) [97]. Non-aqueous suspensions can be modified by adding charging agents and dispersants such as molecular iodine [76, 98], polyethyleneimine (PEI) [40], N-butylamine [99], and etc. The generally accepted scheme of the influence of molecular iodine on the zeta potential is the generation of protons in the suspension by reacting with acetylacetone or alcohol in a dispersion medium, which leads to a zeta potential increasing according to [76]. Methodology for the selection of a charging agent based on its effect on the zeta potential/pH curve, on the isoelectric point and on the ionic conductivity of the suspension of ceramic particles was given in [100]. It worth noting that suspensions based on weakly aggregated nanosized powders obtained by electric explosion of a wire (EEW) [101, 102], and also by laser evaporation with the following condensation (LEC) [103, 104], exhibit high zeta potential (more than 26 mV in the absolute value),

which ensures stability of the suspensions without using dispersants and charging agents [78]. In such the suspensions, a high zeta potential is associated with the self-stabilization effect that arises due to the dissociation of metal cations on the surface of nanoparticles in a liquid medium [105]. Polymeric binders are often added in suspensions to eliminate coatings cracking during their drying, e.g. BMMA-5 (butyl methacrylate copolymer with 5 mole % methacrylic acid), polyvinyl butyral (PVB), polyacrylic acid, polyvinyl acetate, PEI, acrylic acid-acrylate and acrylate-acrylamide copolymers, para-hydroxybenzoic acid (PHBA), and etc. [40, 63, 75, 106].

2.3. Deposition process

The EPD process can be divided into two stages: (1) migration of charged particles in the suspension to the deposition electrode, and (2) destabilization of particles followed by deposition on the electrode surface.

Figure 3 illustrates the most accepted mechanism of EPD connected with the changing EDL structure around the particles and their coagulation near the electrode surface, proposed by Sarkar&Nicholson [32]. The movement of charged particles in a suspension under the influence of the applied electric field causes EDLs distortion, expressed in elongating in the direction of movement and “tail” formation at the opposite side. The movement of ions, co-directed to the particles’ movement, leads to a change in the concentration of counterions in a diffuse part of the EDL of particles near the electrode. This results in reducing the EDL thickness and decreasing the potential repulsion barrier of the particles, causing coagulation followed by deposition. Different others destabilization mechanisms causing deposition were proposed in literature: due to particle accumulating and flocculating near the electrode [107], changing pH at the electrode/solution interface [108], neutralizing the particles charge on the electrode [109], electrochemical coagulating [110], and etc.

Depending on the sign of the zeta potential, cathode and anode EPD can be distinguished - when particles in suspension move towards the cathode (with a positive zeta potential) or towards the anode (with a negative zeta potential). Commonly, for EPD of ceramic materials, particularly SOFC functional layers, substrates for the deposition are placed on the cathode, thereby realizing cathodic EPD [38]. In term of electrical regimes of EPD, the deposition can be performed at the constant voltage or current [111], as well as at the alternating and pulsed voltages [112].

Installations for conducting EPD are cost-effective and simple. They comprise the following main components: a voltage (current) source, a container with

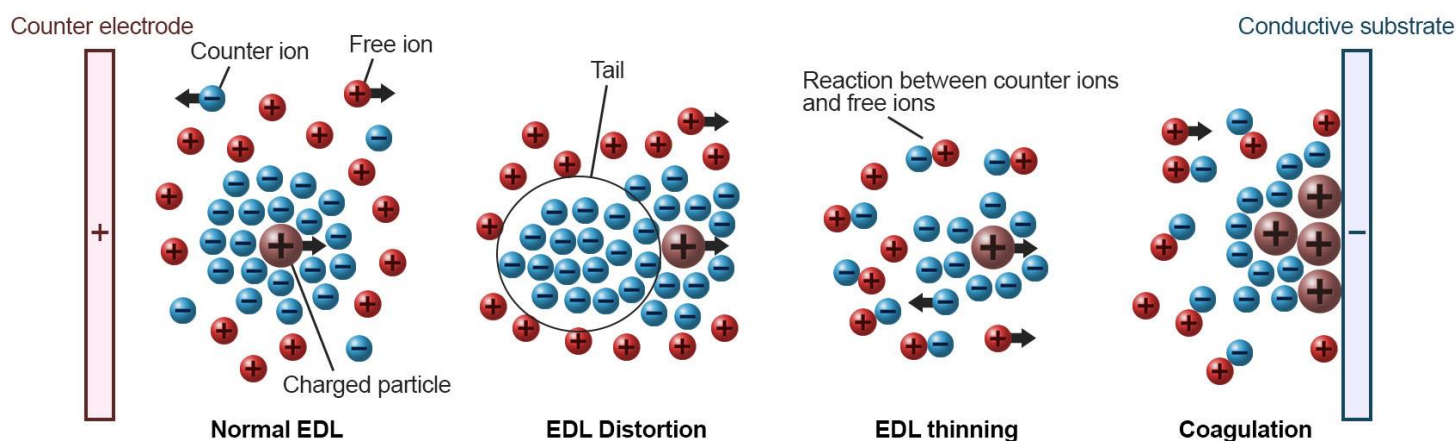


Figure 3 Schematic representation of the deposition mechanism changing the structure of the particles EDLs under the external electric field followed by coagulating.

a suspension, and electrodes (anode, cathode). Installations for the EPD of functional layers for planar SOFCs can be organized with vertical or horizontal electrodes. In EPD installations with the horizontal arrangement of the electrodes, EPD can be implemented on the upper electrode or on the lower electrode [113]. When depositing on the upper electrode, the particle movement occurs against gravity. In this case the suspensions with a broad particle size distribution can be used, since large particles and agglomerates will be subjected to sedimentation, and the resulting coating will be represented by smaller particles. For the manufacture of tubular SOFCs, the EPD installations are organized with a cylindrical counter electrode and deposition is carried out on a coaxially mounted central electrode. Planar installations were successfully used for the deposition of dense electrolyte layers, including multilayer or composite structures deposited on porous cathodes, anodes or dense electrolyte substrates [54, 76, 114, 115], barrier and protective layers [83, 116, 117], porous electrodes [118–120]. Cylindrical EPD installations were adopted for the formation of functional layers, half cells or full structures of microtubular SOFCs [58, 86, 121]. Figure 4 presents examples of various SOFC structures obtained using planar and cylindrical EPD installations.

2.4. EPD: Pros and Cons

Overall, the EPD has the following advantages: there is no need to use expensive equipment, in contrast to RF and magnetron sputtering, pulsed laser and atomic layer deposition and majority of others physical and chemical methods [27]; preservation of the deposited coatings stoichiometry, and possibility of depositing films of complex compositions [47, 79, 122]; deposition can be carried out on substrates with an arbitrary shape, including tubular ones [86, 123, 124]; high deposition rate (up to 10 microns in one minute) [30]; high density of

green coatings (40–60 % of the theoretical value) [125]; the ability to precise control the coating thickness by changing the deposition modes (voltage, time) [32, 126]; good adhesion of the deposited layers to each other and to the substrate [79, 127].

The method finds its application not only for forming coatings, but also for creating bulk samples (compacts) a few millimeters thick [129–131].

Limitations of the EPD method are related to the need to use a conductive substrate. However, successful electrophoretic deposition on porous non-conductive substrates as well as on dense non-conductive substrates, is possible by creating a conductive sublayer on their surface [132, 133]. Moreover, the deposition on highly porous, non-conductive substrates can be implemented according to the mechanism of electrophoretic filtration on the substrates with the porosity more than 50 % [134]. In this case, the deposition can be performed without conductive sublayers, directly on a substrate, which prevents possible coating delamination during their burning out.

The thickness of the coatings when using the EPD method is limited by the particle size of the applied powder. Micro-sized powders can be used for the coatings with thicknesses higher than 10 μm [45], while for nanosized powders the coating thickness can be reduced to 1–2 μm or less [47, 114]. However, in the case of using nanosized powders, the pores size on the substrate surface should not exceed 1 μm [42].

An important feature of the EPD method using for creating ceramic coatings is the deposited coatings drying and their subsequent high-temperature sintering, which can be accompanied by shrinkage, interdiffusion, chemical interaction between the film and the substrate [81, 135]. The integrity and gas tightness of the coating can be ensured by matching the shrinkage and coefficient of

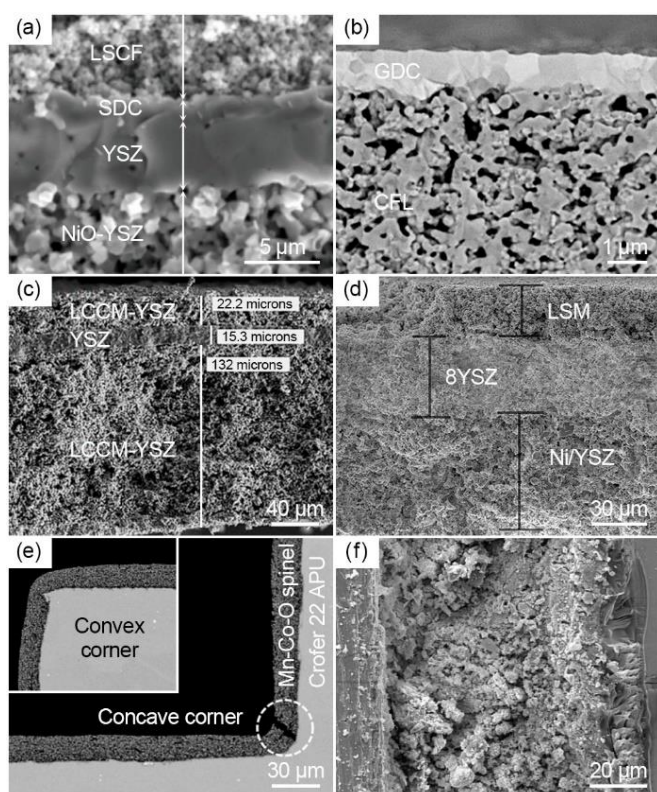


Figure 4 Examples of SOFC structures formed using EPD: (a) bilayer YSZ/Sm-doped CeO₂ (SDC) electrolyte on the supporting NiO-YSZ anode [114]; (b) single-layer Gd-doped Ceria (GDC) film on a (La_{0.8}Sr_{0.2})_{0.95}Co_{0.2}Fe_{0.8}O_{3-δ} (LSCF) cathode support [88]; (c) symmetrical microtubular SOFC with thin film YSZ electrolyte and La_{0.7}Ca_{0.3}Cr_{0.8}Mn_{0.2}O_{3-δ}-YSZ composite electrodes [128]; (d) microtubular anode-supported SOFC obtained by EPD by deposition of anode, electrolyte and cathode for 20 s, 45 s, 20 s [58]; (e) protective spinel layer deposited on a complex-shaped interconnector [116]; (f) functionally graded NiO-YSZ anode obtained by EPD [120].

thermal expansion (CTE) of the electrode/electrolyte materials during sintering [115, 136, 137].

3. Peculiarities of electrophoretic deposition of oxygen-ion and proton conducting electrolytes

3.1. Deposition of thin ZrO₂-based electrolyte films on electrode substrates

The very first work on the use of EPD for SOFC technology was carried out by the Ishihara group to deposit layers of YSZ, a solid electrolyte developed for high temperature fuel cell applications, on porous anode and cathode substrates [67, 138]. Initially, dense YSZ layers ~5 μm thick were obtained on a porous NiO-Zr(Ca)O₂ anode by sintering at a temperature of 1375 °C, 1 hour. To ensure EPD, anode substrates were plated with Pt, which also served as an anode collector in further experiments in the SOFC mode. EPD was performed at a constant voltage 10 V, 3 min. The occurrence of through pores in the coating due to the influence of the porous structure of the

substrate was noted. This problem was overcome using cyclic EPD, in which several cycles of deposition-sintering were carried out. An increase in the open circuit voltage (OCV) value and maximum power density (MPD) was noted with an increase in the number of deposition-sintering cycles. Further work by Ishihara et al. was directed to the deposition on conducting porous La_{0.8}Sr_{0.2}MnO₃ (LSM) substrates ($T_{\text{sint}} = 1350\text{ °C}$) [138]. To obtain dense coatings up to 15 μm thick, six deposition-sintering cycles was performed. Based on the results of testing the YSZ/LSM cells in the SOFC mode at 1000 °C, it was shown that that optimal sintering temperature of the deposited YSZ film was 1300 °C (6 h) which resulted in OCV ~1.0 V and MPD 1.5 W/cm², while further increasing the sintering temperature reduced the cell performance due to the formation of the secondary phase of La₂Zr₂O₇.

In the studies initiated by M. Liu group [76, 139], the dense YSZ films 10 μm thick were obtained on porous LSM and LSM-YSZ substrates by co-sintering at a temperature of 1250 °C, 3 h. Characteristic features of this work were the use of a single-cycle EPD and densification of YSZ at a reduced temperature, facilitated by shrinking the substrates, the pre-sintering temperature of which was reduced to 700 °C.

The influence of the surface modification of LSM-based tubular substrates on the uniformity of their conductive properties and quality of YSZ films obtained by EPD was investigated in the studies performed by Basu et al. group [121, 140]. The deposition of carbon layers by pyrolytic decomposition of propylene (CVD deposition) was shown to decrease conductivity of the substrate. Dense sintered YSZ films were obtained at a sintering temperature of 1350 °C; however, in some cases, the coating cracked depending on the CVD carbon deposition modes. Graphite coating obtained by sputtering improved the uniformity of the conductive properties of the porous LSM substrates. The authors demonstrated potential benefits of burnable carbon coatings in improving the quality of the YSZ films due to reducing the effect of film and substrate shrinkage mismatch during co-sintering.

Despite the advantages associated with deposition on conductive cathode substrates, a lot of effort was invested in the development of electrophoretic deposition for anode-supported SOFCs with a reduced operating temperature [141]. The common way to ensure surface conductivity of non-conductive NiO-cermet anodes was the deposition of conductive (for instance, graphite) layers by painting [142, 143] or spraying [132]. In a number of studies, EPD of YSZ films on reduced anode substrates was considered [40, 71, 89].

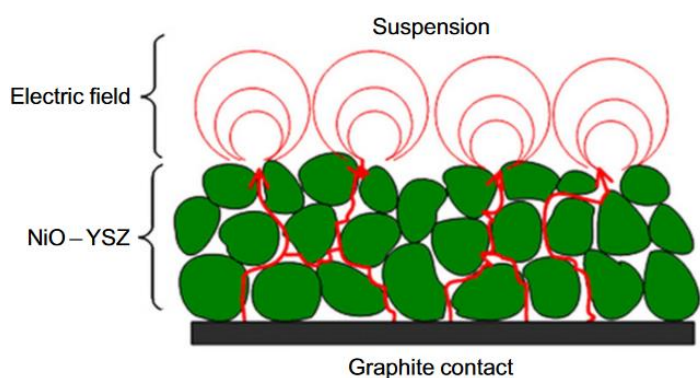


Figure 5 Schematic view of the mechanism of EPD on non-conducting highly porous substrates [11].

Carrying out direct EPD of the YSZ layer on non-conductive NiO-YSZ anode substrates was proposed by Besra et al. group [68, 134]. The authors discussed a charge transfer mechanism during the deposition of an electrolyte film through the porous structure of a substrate filled with a suspension. The presence of continuous pores in substrates (50–70 %), when saturated with a solvent, promotes the formation of “conducting paths” between the electrode and particles in suspension (Figure 5).

At a given applied voltage, there is a threshold value of porosity below which EPD becomes practically impossible. Specifically, to conduct direct EPD, the NiO-YSZ substrates were pre-sintered at 1000 °C for 4 h, the substrate porosity was as high as 72.5 %. A YSZ film 40 μm thick was deposited at 100 V for 3 min and sintered at a temperature of 1400 °C for 2 h. The use a carbon sheet connected with a power source as an electrode allowed deposition at a relatively low voltage compared to the direct EPD on non-conductive substrate covered with carbon proposed earlier by Matsuda et al. (at 400–900 V) [144].

The method of direct EPD found its further developed in the studies of Das&Basu group [91, 145]. It was established that coatings can be obtained by deposition on a substrate up to 1 mm thick. The influence of the substrate thickness can be associated with an uneven distribution of the electric field strength in the case of the substrate thickness more than 1 mm. The authors considered the possibility of obtaining by direct EPD of thin $\sim 3 \mu\text{m}$ YSZ films using a nanosized powder synthesized by a sol-gel method [55]. YSZ films were

directly deposited at the applied voltage of 10–70 V for 1–6 min onto the porous non-conducting NiO-YSZ anodes using a conducting steel plate on the reverse side of the substrates and co-sintered with the substrates at a temperature of 1200 °C for 2 h. The SEM analysis confirmed film dense structure and good adhesion to the highly-porous anode substrate. As nanosized powders prone to agglomeration, a specific scheme of a stable suspension preparation can be proposed for such the materials (Figure 6), as it was revealed in [55].

The charging method that uses the mixture of ethanol and acetylacetonate was applied by Xu et al. [146] to stabilize the suspensions of YSZ nanoparticles (20–30 nm). As a result, dense YSZ coatings on a porous LSM cathode were obtained at 1300 °C. Meepho et al. obtained dense YSZ coating from nanosized powder produced via solvothermal procedure ($\sim 5 \text{ nm}$) on porous NiO-YSZ substrates from ethanol based suspension modified with 1,3-propanediol [147]. To retain the porous structure of the anodes, prepared using both commercial and homemade YSZ, the sintering temperature of the deposited coatings did not exceed 1400 °C. The use of weakly aggregated YSZ nanosized powders (mean size of 10.9 nm) obtained by laser evaporation and condensation (LEC) method allowed depositing dense electrolyte layers with a thickness of less than 5 μm on LSM substrates by Kalinina et al. group [42, 44]. A feature of YSZ-LEC suspensions was the spontaneous formation of a high zeta potential due to a self-stabilization effect. It was established that for the successful deposition on nanosized LEC-powder, the pore sizes on the substrate surface should not exceed 1 μm . A decrease in the size of large pores on the surface of the LSM cathode substrates was achieved by preliminary EPD of a microsized LSM powder followed by deposition of YSZ-LEC [42].

The target SOFC parameters are the open circuit voltage (OCV) and the maximum power density (MPD), which are achieved by optimization of the cell design, the choice of the substrate, the thickness of the electrolyte membrane and its gas-tightness. Examples of the performance characteristics of SOFCs with zirconia-based electrolytes produced by EPD are presented in Table 2. The information of the size of the substrates and the deposited film thickness is also shown.

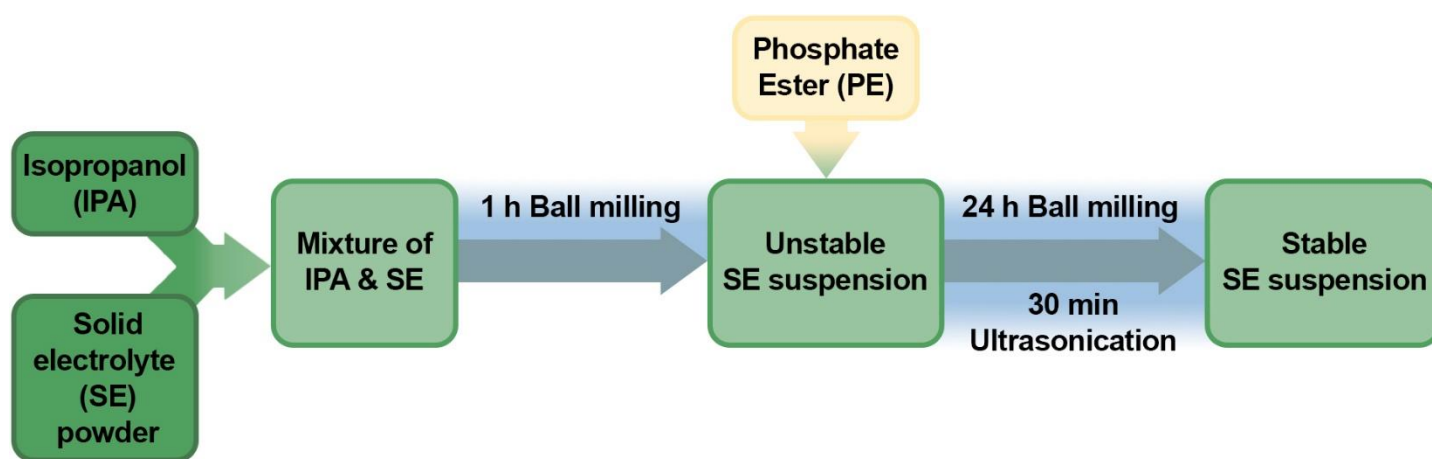


Figure 6 Schematic presentation of the specific process of preparation of a stable suspension based on nanosized powers.

3.2. Electrophoretic deposition of oxygen-ion conducting electrolytes for SOFCs operating in IT range

Development of effectively functioning Intermediate Temperature Solid Oxide Fuel Cells (IT-SOFCs) is a highly relevant task, which attracts increasing attention of a broad *R&D* community [152]. However, as SOFC functional layers are represented mainly by oxide materials, a decrease in temperature leads to resistivity and electrochemical activity issues both for electrolyte materials and electrodes. The problem of maintaining SOFC efficiency at lower operating temperatures can be partially solved by searching for new highly conductive electrolytes [153, 154].

Particularly, application of solid electrolytes with a fluorite structure based on doped CeO_2 , highly conductive in the intermediate temperature range, allows reduction of the cell operating temperature down to 700 °C without loss of efficiency due to increasing the ohmic electrolyte resistance [11]. The level of electronic conductivity due to partial reduction $\text{Ce}^{4+} \rightarrow \text{Ce}^{3+}$ in CeO_2 -electrolyte, which causes decreasing SOFC efficiency, can be reduced by proper co-doping with rare-earth and alkali-earth elements, especially with Ba [155]. Sc-doped ZrO_2 , co-doped with other rare-earth elements to improve phase stability at decreased temperatures, also give advantages compared to YSZ when using in IT-SOFC [156]. The promising electrolyte candidate for the devices operating in the IT range – solid state electrolytes with a perovskite structure based on LaGaO_3 and LaAlO_3 substituted on the A- and B-sites with enhanced oxygen ionic conductivity [9]. Other ionic-conducting oxides with an apatite structure based on $\text{La}_{10}\text{Si}_6\text{O}_{26}$ composition also can of interest from the point of view of low-cost, high abundance materials [157]. Unfortunately, a drawback of apatite-like materials is the high temperatures required for their densification, therefore, alternative synthesis and

Table 2 – Performance of SOFCs with YSZ electrolyte membranes formed by EPD on supporting electrodes.

Substrate, shape/size, T_{sint} (°C)	Electrolyte, thickness, T_{sint} (°C)	OCV (V)/MPD (W/cm ²) T (°C)	Refs
NiO-Zr(Ca)O ₂ disk, 20/1 mm 1450	YSZ 5 μm 1400	1.03/1.84/1000 (H ₂ +H ₂ O/O ₂)	[67]
NiO-YSZ disk, 12.15-12.82/0.68-0.95 mm 1000	YSZ 10 μm 1400	0.86/0.264/850 0.97/0.060/650	[134]
NiO-YSZ disk, 19/0.7 mm 900	YSZ 5 μm 1400	1.094/1.02/800 1.131/0.19/600	[144]
NiO-YSZ+ CMS ^a disk, 10/0.8 mm 1000	YSZ 12 μm 1400	0.96/0.202/850 With CMS (5%): 1.078/0.572/850	[148] [149]
NiO-YSZ disk, 12.15-12.82/0.68-0.95 mm 1000	YSZ 40 μm 1400	0.86/0.264/850 0.97/0.050/650	[134]
NiO-YSZ ^{PIM} ^b green disk, 20/1.5 mm	YSZ 3 μm 1250	1.06/0.040/800	[51]
NiO-YSZ(nano) disk, 16/ 1.5 mm 900	YSZ 3 μm 1200	1.05/0.90/800 1.07/0.65/700	[55]
Graphite road NiO-YSZ (tube)	YSZ 5.7 μm 1400	1.10/0.30/750 112/0.21/700	[150]
Full μ-SOFC by EPD (tube)	YSZ 6 μm	0.180/0.003/800 10%H ₂ in N ₂ /air	[124]
La _{0.8} Sr _{0.2} MnO _{3-δ} plate, 4 cm ² 1350	YSZ 10 μm 1275	1.00/1.50/1000 (H ₂ +H ₂ O/O ₂)	[138]
La _{0.7} Sr _{0.3} MnO _{3-δ} (nano/mic 50:50) disk, 15 mm 900-1200	Zr _{0.1} Y _{0.9} O _{1.95} 5 μm 1250	1.1/0.55/850 0.40/750 0.15/650	[151]

^a – microsphere;

^b – powder injection molding.

densification methods (including deposition as thin films) are key areas of development for their practical application.

The use of the electrophoretic deposition method in obtaining thin-film coatings based on the electrolytes developed for IT-SOFCs in less developed compared to the deposition of YSZ films. A number of works was done using green anode substrates fabricated with addition of graphite (carbon) to make them suitable for deposition. Nakayama&Miyayama [72] performed EPD of Sm-doped ceria (SDC) on a carbon-filled NiO–SDC cermet substrate followed by co-sintering at 1400 °C, 25 h. As a result, a dense SDC film with a thickness of ~8 μm was obtained. Film and substrate shrinkage compatibility during co-sintering was controlled by the amount of carbon added to the substrate and the particle size of the cermet powder. At a NiO–SDC particle size of 49 nm, the optimal carbon content was found to be equal to 9 wt. %.

Ichiboshi et. al [62] produced single-layer SDC coatings on Ni–SDC cermet substrates with the addition of graphite in a ratio to the cermet powder 1:1 (wt %). After sintering at a temperature of 1600 °C for 10 h, an SDC film with a thickness of ~20 μm was obtained. The SDC coating contained pores and microcracks, therefore the achieved SOFC performance was not high.

Cheng et al. [158] carried out the formation of an SDC electrolyte layer on NiO–SDC substrates to obtain a single-chamber SOFC cell for operation in a methane-air mixture. The authors chose the optimal composition of the SDC suspension (concentration 5 g/L, powder particle size 248 nm) and obtained an SDC film 18 μm thick by sintering at a temperature of 1350 °C for 12 h. The authors argue that when deposited from a less concentrated suspension, a denser packing of particles in the coating can be obtained, which improves the characteristics and performance of the resulting SOFC cell.

Kalinina et al. group carried out a series of studies on the deposition of CeO₂-based electrolytes both on cathode and anode substrates. Particularly, EPD of single-layer coatings based on multi-doped solid electrolyte Ce_{0.8}(Sm_{0.75}Sr_{0.2}Ba_{0.05})_{0.2}O_{2-δ} (CSSBO) on dense La₂NiO_{4+δ} (LNO) and porous multilayer LaNi_{0.6}Fe_{0.4}O_{3-δ} (LNFO)/LNO cathode substrates was performed in [47, 79]. A feature of these works was the use of CSSBO nanosized powder obtained by the LEC method, the suspensions of which were characterized by the effect of self-stabilization. Dense sintered CSSBO coatings 2 μm thick were obtained on the dense LNO at a sintering temperature of 1400 °C for 5 h. The total conductivity of the coating was 0.1 S/cm at 650 °C (activation energy 0.76 eV). It was shown that to eliminate pores in a CSSBO

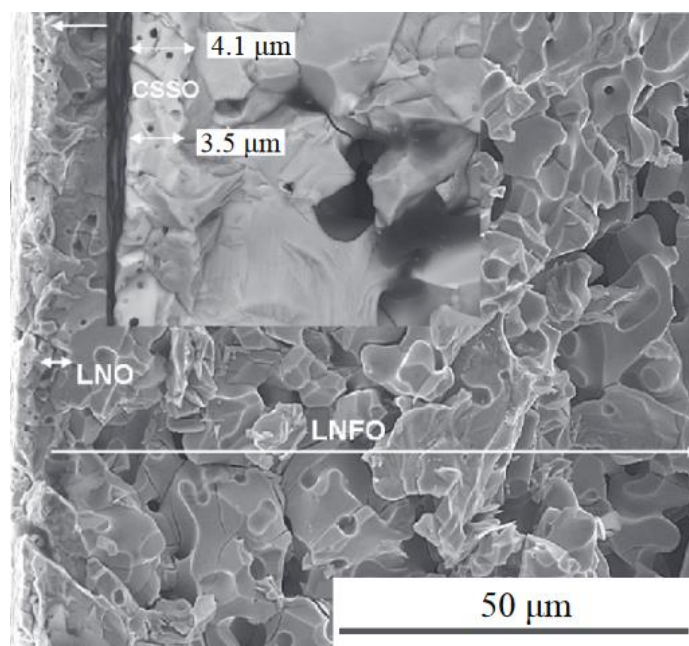


Figure 7 Electron micrographs of the resulting half-cell with a deposited layer of the CSSO electrolyte, functional LNO layer, and LNFO collector (from left to right). Reproduced with permission [80]; Copyright 2019, Pleiades Publishing.

film deposited on LNFO/LNO multilayer substrates, it was necessary to perform several deposition-sintering cycles. In this case, the conductivity of the film was lower than that for single deposition on a dense substrate and amounted $2.40 \cdot 10^{-2}$ S/cm at 750 °C. Similar deposition procedure was applied for the deposition of Ce_{0.8}(Sm_{0.8}Sr_{0.2})_{0.2}O_{2-δ} (CSSO) on the LNFO/LNO substrate with optimized porosity (Figure 7). The dense electrolyte film was obtained 1400 °C for 4 h. This temperature did not exceed the sintering temperature of the collector layer; thus, its structure and gas permeability were preserved.

Various options for creating electrical conductivity of the cermet anode substrates were considered by Kalinina&Pikalova group, namely, the reduction of cermet substrates in a hydrogen-argon mixture; deposition of a conductive sublayer of finely dispersed platinum (20 μm) on the front side; synthesis of a conductive polymer layer - polypyrrole (PPy); infiltration into the porous structure of the anode of an aqueous solution of silver nitrate, followed by centrifugation and annealing [135, 159]. The NiO–SDC substrates used for the studies were pre-sintered at 1400 °C for 2 h. It was shown that during EPD, continuous SDC coating was formed on the reduced Ni-SDC substrate, however subsequent high-temperature sintering in an oxidizing atmosphere at a temperature of 1400 °C for 5 h led to the complete destruction of the SDC coating, while maintaining the integrity of the NiO–SDC substrate. This effect is due to significant internal mechanical stresses associated with a change in the specific volume during the oxidation of the

reduced cermet substrate. A more successful option for implementing the formation of an SDC solid electrolyte layer was the use of deposition of a platinum sublayer (20 μm) on a nonconductive cermet substrate. After cyclic EPD (4 cycles) and final sintering at 1500 $^{\circ}\text{C}$ for 5 h, a dense sintered 40 μm thick SDC coating with closed porosity was obtained. It is important to note that no diffusion penetration of platinum into the sintered SDC electrolyte layer occurred.

One of the important tasks in the implementation of the electrophoretic deposition of solid electrolytes on porous substrates is to achieve the lowest possible coating sintering temperature in order to preserve the porous structure of the electrode and its high electrochemical activity at a reduced operating temperature. In the study performed by Kalinina&Pikalova group [160], to enhance sintering properties of SDC films, directly deposited on highly porous non-conductive NiO–BaCe_{0.8}Sm_{0.2}O₃ (BCS) and NiO–SDC substrates, introducing Co₃O₄, TiO₂, and Al₂O₃ oxides in the amount of 2, 2 and 5 mol. % was used. Dense electrolyte membranes up to 30 μm in thickness were obtained after sintering at 1450 $^{\circ}\text{C}$ for 5 h. In SOFC mode, the increasing the open circuit voltage (OCV) (1.06–0.92 V at the temperatures of 650–750 $^{\circ}\text{C}$) was demonstrated as a consequence of the formation of a Ba-rich layer on the interface caused by the diffusion from the NiO–BCS substrate during sintering. It should be noted, that at 1450 $^{\circ}\text{C}$, complete densification of Co-modified SDC films on the NiO–SDC anode substrate did not occur. The authors argue that the sintering properties are influenced by both the Ba diffusion and the sintering additives. Stabilization of the suspensions based on SDC-micropowder with oxide additives used in the study was achieved by introducing the SDC–LEC powder in the amount of 10 wt % according to a “halo” mechanism, earlier described in [161, 162].

A significant improvement in the sinterability of a GDC-based electrolyte film was demonstrated by Yamamoto et al. [88] using cubic GDC nanoparticles obtained by hydrothermal synthesis. EPD was carried out on a pre-sintered porous cathode (La_{0.6}Sr_{0.4})_{0.95}Co_{0.2}Fe_{0.8}O_{3- δ} (LSCF) at 1100 $^{\circ}\text{C}$, 2 h. To implement deposition from an aqueous suspension of GDC nanopowder, a complex composition of additives was used comprising PAAA as a dispersant, methylcellulose as a binder, polyethylene glycol as a plasticizer, and 1-octanol as a defoamer to suppress bubbles formation. A GDC film 1 μm thick was obtained by sintering at a temperature of 1000 $^{\circ}\text{C}$ for 2 h.

In the studies of X. Liu group, the aqueous deposition of a commercially available Gd-doped CeO₂ was

developed [87]. The authors deposited cathode barrier layers based on Gd-doped CeO₂ on a YSZ electrolyte to suppress its interaction with LSCF cathode [60]. YSZ surface was coated with polypyrrole (PPy) as the conductive agent. GDC barrier layers ranging in thickness from 5 μm to 8 μm were successfully densified at temperatures as low as 1300 $^{\circ}\text{C}$. The same group implemented alternating current EPD (AC-EPD) of GDC on half-cell comprising NiO–YSZ/YSZ, pre-sintered at 1250 $^{\circ}\text{C}$ [163]. The voltage waveform consisted of negative and positive voltage steps of varying magnitude and step length. The optimum frequency of 500 Hz leads to the maximum deposition yield. A bilayer electrolyte YSZ (10 μm)/GDC (6 μm) was obtained by sintering at a temperature of 1250 $^{\circ}\text{C}$ for 4 h. The authors managed to reduce the sintering temperature by introducing a sintering additive in the amount of 2 mol % FeO_{1.5}. The authors attribute the improvement in coating density to a decrease in the generation of molecular hydrogen near the substrate due to using AC-EPD.

The possibility of obtaining two-layer YSZ/SDC electrolytes on pre-sintered porous NiO–YSZ anode substrates at a temperature of 900 $^{\circ}\text{C}$ was shown by Matsuda et al. [114]. EPD was performed by electrophoretic filtration on highly porous substrates covered with graphite layer on the back side. Subsequent deposition of YSZ and SDC layers was performed at 600 V. The obtained films were co-sintered with the anode at 1400 $^{\circ}\text{C}$ for 2 h. To avoid delamination of the two-layer electrolyte during sintering, the thickness of the SDC layer was decreased down to 1 μm .

Yamaji et al. group [59,164] carried out EPD of Sc₂O₃ doped ZrO₂-based (SSZ) films on NiO–SSZ substrates prepared by mixing of graphite in the amount up to 40 wt. % with the cermet material. A thin (5–8 μm thick) SSZ electrolyte was dense enough when co-sintering temperature was set at 1275 $^{\circ}\text{C}$. It was found, that cracks formed in the electrolyte film during the co-sintering process, when the shrinkage of the anode substrate was smaller than that of the electrolyte. The mismatch in shrinkage was controlled by changing the preparation conditions for the anode substrates, amount of graphite and starch powders.

Thin films of La_{1-x}Sr_xGa_{1-y}Mg_yO_{3-(x+y)/2} were prepared by cyclic EPD from an acetone-based suspension with addition of J₂ in [165]. Dense films with uniform thickness of 4 μm were obtained on the Pt substrates after five cycles of deposition/sintering at 1400 $^{\circ}\text{C}$ for 1 h. The conductivity of the films was approximately 0.12 S/cm at 775 $^{\circ}\text{C}$, which was close to the conductivity of the relative bulk samples. In [41], La_{0.83}Sr_{0.17}Ga_{0.83}Mg_{0.17}O_{2.83}

electrolyte films were obtained by one-step EPD on conducting Pt and LSM substrates from suspensions based on a mixed acetone/ethanol dispersion medium and sintered at 1300 °C. It was found that LSGM films 10–20 μm thick exhibited good adhesion to the Pt substrate, while those deposited on LSM exhibited cracking after sintering. The bulk conductivity of the Pt supported LSGM film showed the same behavior as that of the compact LSGM electrolyte ($E_a = 0.93$ eV and 0.99 eV, respectively). The LSGM film exhibited lower bulk electrical conductivity than the latter ($4.1 \cdot 10^{-3}$ and $4.4 \cdot 10^{-2}$ S/cm, respectively, at 700 °C). This difference should be ascribed to the slight Ga depletion in the LSGM film during deposition and sintering.

As in the case of YSZ, CeO₂-based barrier layers are often used to prevent interaction LGSMElectrolyte with perovskite cathodes and cermet anodes [9]. A three-layer GDC/La_{0.8}Sr_{0.2}Ga_{0.8}Mg_{0.2}O_{3-δ} (LSGM8282)/GDC electrolyte was obtained by Suzuki et al. [133] with a layer thickness of ~15 μm on a porous NiO-YSZ anode substrate using a conductive polypyrrole sublayer. Despite the high OCV value (1.112 V at a temperature of 600 °C), the achieved MPD was very low, 0.011 W/cm² at a temperature of 800 °C, which the authors attributed to the formation of secondary phases due to chemical interaction of GDC and LSGM during sintering.

La-doped CeO₂ was found to be more compatible with LGSMElectrolytes [9]. Bozza et al. [166] carried out one-step EPD of a LSGM8282 electrolyte on tape-cast composite electrodes, composed of La-doped ceria (LDC), polyvinylidene difluoride (PVDF) and carbon powders. A dense 15 μm thick electrolyte film was obtained by co-firing at 1490 °C, with preservation the substrate porous structure (Figure 8). Moreover, the EDS analyses revealed negligible interaction between perovskite and fluorite phases (inset in Figure 8).

EPD of apatite-type electrolytes is still in its initial stage of development. Jothinathan et al. [64] reported on EPD of La_{9.83}Si_{4.5}Al_{1.5}O₂₆ (LASO) electrolyte prepared by a modified sol-gel procedure on porous LASO-NiO anode substrates. To perform direct deposition on cermet anodes, pre-sintered at 1300 °C, the authors used a modified electrode set-up combining a conductive ring with an insulating backing plate. The thick uniform deposit of 25 μm was formed after 50 s at 150 V. Suarez et al. reported on EPD of La_{9.33}Si₆O₂₆ electrolyte films from ethanol-based suspensions modified with PEI [63]. Highly dense film (99.1 %) with a Vickers hardness of 7.57 GPa was obtained by sintering at 1500 °C for 10 h.

Finally, Table 3 summarizes the studies on testing in SOFC mode of the cells with oxygen-ion conducting films, including bilayer structures.

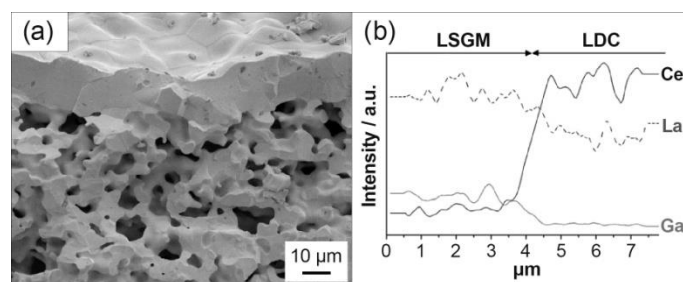


Figure 8 (a) SEM micrograph of the cross section of the dense LSGM film supported on a porous LDC substrate and (b) EDS line profile analysis across the LSGM/LDC interface. Reproduced with permission [166]; Copyright 2008, John Wiley and Sons.

Table 3 – Performance characteristics of IT-SOFCs with oxygen-ion conducting electrolyte membranes formed by EPD.

Substrate (T_{sint} , °C)	Electrolyte (T_{sint} , °C)	OCV (V)/MPD (W/cm ²) T (°C)	Refs
NiO-SDC+graphite 9 wt % disk, 15 mm	SDC 8 μm 1400	0.7/0.272/700 0.281/600 0.161/500	[72]
NiO-SDC+graphite	SDC 20 μm 1600	0.61/0.072/700	[62]
NiO-SDC disk, 16 mm	SDC 18 μm 1350	0.95/0.155/500 CH ₄	[158]
NiO-BCS disks 15/1 mm	SDC/Ti 30 μm SDC+Al 27 μm SDC+Co 20 μm	1.00/0.122/750 0.98/0.125/750 0.92/0.101/750	[160]
NiO-YSZ/YSZ 1250 h = 0.4 mm	SDC/Fe 6 μm 1250 AC-EPD	0.75/750 0.52/700 0.31/650	[163]
NiO-YSZ 900	YSZ 4 μm / SDC 1 μm 1400	1.1/0.61/700	[114]
NiO-SSZ + graphite disks, 22/2 mm	SSZ 8 μm 1275	1.113/0.440/750 1.117/0.270/700	[164]
NiO-SSZ 900 red 600 h = 0.7 mm	SSZ 10 μm 1300	1.0-1.1/1.8/900 0.4/700	[71]
NiO-YSZ 900	GDC 15 μm/ LSGM 15 μm/ GDC 15 μm 1400	0.95/0.011/800 1.05/0.009/700 1.112/0.005/600	[133]

3.3. EPD of proton-conducting electrolytes on supporting dense and porous substrates for IT-SOFCs

Proton-conducting electrolytes based on doped barium cerate/zirconate are promising for the use in SOFCs due to a sufficiently high level of co-ionic (proton and oxygen-ion) conductivity [167]. One of the main difficulties that arise in the formation of proton-conducting electrolyte membranes based on BaCeO_3 is the evaporation of barium during high-temperature sintering, which causes films' deficiency in terms of barium content, and deterioration of their sinterability and conductivity. Ba evaporation was observed for both volume samples and films [168–170]. It became more pronounced at increased sintering temperatures and also for films with a thickness of less than 10 microns.

The possibility of implementing EPD of an electrolyte membrane based on $\text{BaCe}_{0.89}\text{Gd}_{0.1}\text{Cu}_{0.01}\text{O}_{3-5}$ (BCGCuO), a perspective proton-conducting electrolyte [171], on supporting cathodes was examined in the works of Kalinina&Pikalova group [81, 82]. The features of preparation of stable suspensions based on microsized powders of doped BaCeO_3 were considered in [45, 172]. Three variants of barium retention in a BCGCuO film were studied [81], namely, the formation of BCGCuO coatings on an $\text{La}_2\text{NiO}_{4+6}$ (LNO) cathode substrate with following sintering in a closed volume with the BCGCuO powder poured around the sample; application of a protective BaCeO_3 (BCO) film deposited on the BCGCuO coating on the LNO cathode; formation of a BCGCuO film on a Ba-modified $\text{La}_{1.7}\text{Ba}_{0.3}\text{NiO}_{4+6}$ (LBNO) cathode. It was shown that the most effective method to preserve Ba in the electrolyte layer was the use of the Ba-modified cathode substrate, which served as a source of Ba during high-temperature sintering. A feature of the application of the EPD method in this work was the use of centrifuged suspensions of microsized BCGCuO with a concentration of 7 g/L in a mixed dispersion medium of isopropanol/acetylacetone (70/30 vol. %) with the addition of a polymeric binder BMMA-5 (copolymer of butyl methacrylate with 5 wt. % methacrylic acid). To obtain a continuous BCGCuO coating 6.6 μm thick, 12 deposition-sintering cycles at a temperature of 1450 $^\circ\text{C}$ for 2 hours were required. According to the EDX analysis, the barium content in the BCGCuO electrolyte film (~19 at. %) was close to the nominal value. Multiple deposition-sintering cycles ensured the "healing" of open pores in the coating (Figure 9). The activation energy of the film conductivity (0.55 eV) was close to that of the compact BCGCuO sample (0.42 eV). However, the conductivity value was lower ($5.5 \cdot 10^{-4}$ S/cm, 600 $^\circ\text{C}$) compared to a compact sample ($6.9 \cdot 10^{-3}$ S/cm, 600 $^\circ\text{C}$),

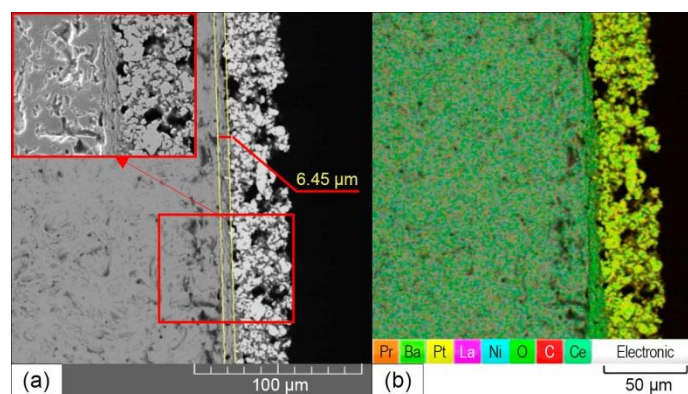


Figure 9 SEM images of the BCGCuO film deposited onto the LBNO substrate after the final sintering at 1450 $^\circ\text{C}$, 2 h: (a) the cross-section of the BCGCuO film on the LBNO (on the left) substrate and Pt electrode (on the right); (b) integrated EDX mapping image of the cross section [81].

due to closed pores in the BCGCuO film caused by multiply deposition, as well as lanthanum diffusion into the electrolyte layer, having a negative effect on the BCGCuO conductivity.

Logical development of the studies performed by Kalinina&Pikalova group was the EPD of the BCGCuO electrolyte film on porous cathode substrates $\text{LaNi}_{0.8}\text{Fe}_{0.4}\text{O}_{3-5}$ (LNFO), LBNO and bilayer cathodes with LNFO carrier/collector layer and a functional LBNO layer. To reduce the number of EPD cycles, a suspension of BCGCuO in an isopropanol/acetylacetone medium (70/30 vol. %) with a concentration of 10 g/L was used with ultrasonic treatment for 125 min without subsequent centrifugation, and also without the addition of a polymer binder. A change in the suspension preparation method made it possible to reduce the number of deposition-sintering cycles from 12 to 5 to deposit a 21 μm thick BCGCuO electrolyte layer. Various approaches to solving the problem of barium retention in the composition of the BCGCuO electrolyte during its sintering were investigated, such as the use of sintering in BaCO_3 powder; the use of a thin functional LBNO sublayer with a thickness of 10 μm , obtained by the EPD method, as well as the use of a barium-modified porous LBNO cathode substrate. It was found that the presence of a bulk LBNO substrate (1 mm thick) and the simultaneous use of BaCO_3 as a protective cover can be an effective way to maintain the Ba content in the BCGCuO electrolyte film 10 μm thick during high-temperature sintering at a temperature of 1450 $^\circ\text{C}$ for 2 hours. Probably, a promising direction in the development of work on the deposition of proton conductors on cathode substrates will be the formation of a multilayer structure of cathodes with a bulk collector (LNFO or other highly conductive electrode material) as well as a Ba-containing functional layer (FL) optimized in

thickness and porosity, which will allow retaining Ba in the electrolyte film and ensure thermomechanical compatibility of the deposited film and substrate during sintering. Among the promising materials for FLs are Ba-doped layered nickelates, which demonstrated excellent compatibility with BaCeO₃-based electrolytes [173–175].

The series of work on EPD of proton-conducting electrolytes, mainly doped BaCeO₃, on anode substrates and their characterization was initiated by the groups of Zunik et al. and Traversa et al. EPD of an BaCe_{0.9}Y_{0.1}O_{3-δ} (BCY10) electrolyte on green NiO-BCY10 anode substrates filled with graphite are represented in [74, 176, 177]. The deposition was carried out from acetylacetonate-based suspensions modified with J₂. With increasing the deposition voltage from 30 to 60 V, the BCY10 film thickness increased from 5.2 μm to 9.5 μm. The lower the deposition voltage, the larger the porosity with larger pinholes and micropores was (Figure 10).

Thus, for the half-cell formation the mode of deposition at 60 V for 1 min was finally chosen. Co-sintering of the electrolyte layer and the anode was done at 1550 °C, 2 hours. The thickness of the BCY10 electrolyte after sintering was 9.5 μm. The OCV value of 1.05 V (700 °C) revealed the gas-tightness of the electrolyte film, the preservation of the porous structure of the anode after sintering was also confirmed. Tests performed on single cells with a composite cathode based on commercial LSCF and synthesized BaCe_{0.9}Yb_{0.1}O_{3-δ} showed, that the performance of BCY10-based cells was mainly limited by the interfacial polarization resistance.

The use of methyl-ethyl-ketone (MEK) with the addition of polyacrylic acid (PAA) for the preparation of suspensions based on BCY10 powder was considered in the work of Argiris et al. [65]. It was shown that with an increase in the amount of PAA to 0.4 wt. %, the negative values of the zeta potential increase to a value of about -40 mV, ensuring the stable EPD process on reduced Ni/BaCe and Ni/YSZ cermets resulting to half cells with green electrolyte layers of 20 μm thickness.

In the work of Itagaki [75] thin layers of the BaCe_{0.8}Y_{0.2}O_{3-δ} (BCY20) solid electrolyte with a thickness of 9.2 μm were obtained by EPD on green NiO-BCY anode substrates filled with graphite. The film was co-sintered with the substrate at 1450 °C. The achieved specific power was significantly lower compared to that obtained for the BCY10-based cell and amounted to 74.2 mW/cm² at 600 °C. The authors attribute the low power value to the high contribution of the electrode polarization resistance.

Doped BaCeO₃-BaZrO₃ proton-conducting materials have been considered recently as a promising electrolytes

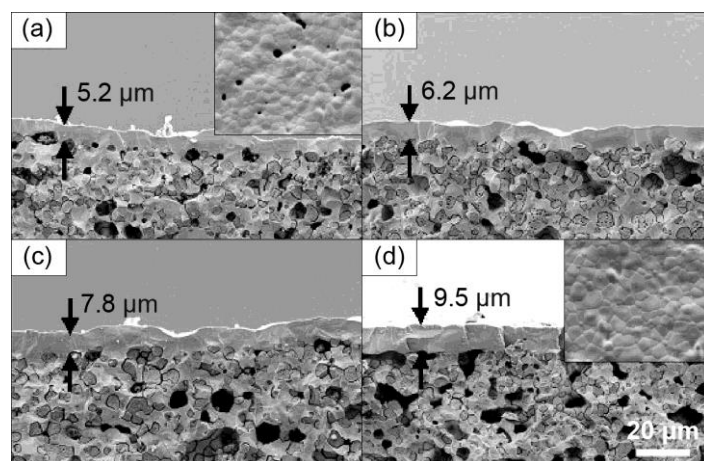


Figure 10 SEM images of the cross section of BCY10 electrolyte membranes on NiO-BCY10 anodes obtained using EPD at various voltages of 30 V (a), 40 V (b), 50 V (c), 60 V (d) after sintering at a temperature of 1550 °C, 2 hours. Reproduced with permission [176]; Copyright 2011, John Wiley and Sons.

for IT-SOFCs and electrolysis cells [178]. The mixed systems combine excellent conducting properties and stability in water and CO₂-containing atmospheres. However, to the best of our knowledge, there are only few studies on EPD of these class of electrolytes. Choudhary et al. [66] studied EPD of a proton-conducting electrolyte of BaZr_{0.4}Ce_{0.4}Y_{0.2}O_{3-δ} (BZCY) on non-conducting porous NiO-BZCY anodes, pre-sintered at 1100 °C for 2 hours (porosity 42.4 %). The deposition was performed from an ethanol-based suspension at 70 V for 2 min. The sintering of the BZCY film with a thickness of ~13 μm was carried out at a temperature of 1500 °C for 2 hours. A decrease in the anode porosity to a value of 19.31 % after sintering was noted.

Kalinina et al. [135] carried out a detailed study of the properties of suspensions based on micro-sized powder of BaZr_{0.3}Ce_{0.5}Y_{0.1}Yb_{0.1}O_{3-δ} (BCZYYbO). Variants of modifying the BCZYYbO suspension by adding molecular iodine (0.4 g/L) and copper oxide (1 wt. %) were studied. It was shown that the addition of iodine did not change the zeta potential of the suspension, the value of which was +7 mV, while the pH shifted to the acid side. However, the addition of iodine made it possible to carry out the EPD process. The BCZYYbO-CuO suspension had a higher zeta potential (+11 mV) and did not require the addition of iodine to carry out the EPD process. The authors argue that the noted features are associated with a change in the mechanisms of EPD with the participation of ions (H⁺ and I⁻) located in the solvate layers around the particles. Previously, an increase in the zeta potential of a suspension upon the addition of iodine was explained by an increase in the zirconia particle charge due to the adsorption of protons generated by the reaction of iodine with acetylacetonate [67, 76, 91]. The absence of any changes

in zeta-potential was also observed when adding iodine to suspensions of various microsized proton-conducting electrolytes [83, 84, 115]. Nevertheless, modification with iodine allowed the stable deposition of microsized powders to be carried out.

Bozza&Bonanos developed EPD of commercially available $\text{La}_{0.995}\text{Ca}_{0.005}\text{NbO}_4$ (LCN) electrolyte on LCN–NiO substrates, prepared by an impregnation method [179]. The deposition was performed from the suspensions based on the mixture of acetylacetone, iodine and water. The developed technique was found to be effective also for the deposition of a mixture of NiO and LCN powders to form anode functional layer. A dense 10 μm thick LCN electrolyte layer and a porous 3 μm thick LCN/NiO anode layer were obtained after co-sintering at 1200 °C.

Direct EPD of a bilayer electrolyte films based on proton-conducting electrolyte $\text{BaCe}_{0.8}\text{Sm}_{0.2}\text{O}_3$ (BCS) and SDC on porous BCS–NiO anode substrates pre-sintered at 1200 °C (porosity 41 %) was performed by Kalinina&Pikalova group [115]. To decrease sintering temperature of the BCS electrolyte, it was modified by the addition of 1 wt. % of CuO. A feature of this work was the use of modified suspensions of microsized SDC powder by adding SDC–LEC nanosized powder (5 wt. %). The use of nanosized powder made it possible to increase the zeta potential from +6 mV to +13 mV, which significantly improved the uniformity of the deposited coatings. The EPD process of BCS–CuO coatings required the addition of molecular iodine (0.4 g/L). The deposition of BCS–CuO and SDC electrolyte layers on non-conducting substrates was carried out at 200 V in one cycle with co-sintering at 1450 °C. The sintering at the chosen temperature resulted in the formation of a composite structure. SEM studies showed that all elements of the composite were evenly distributed throughout its volume (Figure 11 a,b) and there were no individual micron-sized grains related to the barium cerate or cerium oxide phase. Probably, the separation of the phases of the composite electrolyte membrane into the BCS and SDC phases occurred at the submicron level, similarly to that observed by Sun et al. [180].

The OCV value for SOFC cells with BCS–CuO/SDC electrolyte was in the range of 1.05–0.95 V at temperatures of 600–700 °C, which exceeded the OCV value for single-layer SOFC cells with SDC [72] and BCS–SDC (1:1 wt. ratio) [180] electrolytes, demonstrating enhanced effect of blocking the electron leakage current. The analysis of the impedance data showed that the polarization resistance of Pt cathode used for the SOFC testing contributed mostly to the entire cell performance (Figure 12 c). This fact was also stated in [171]. The authors

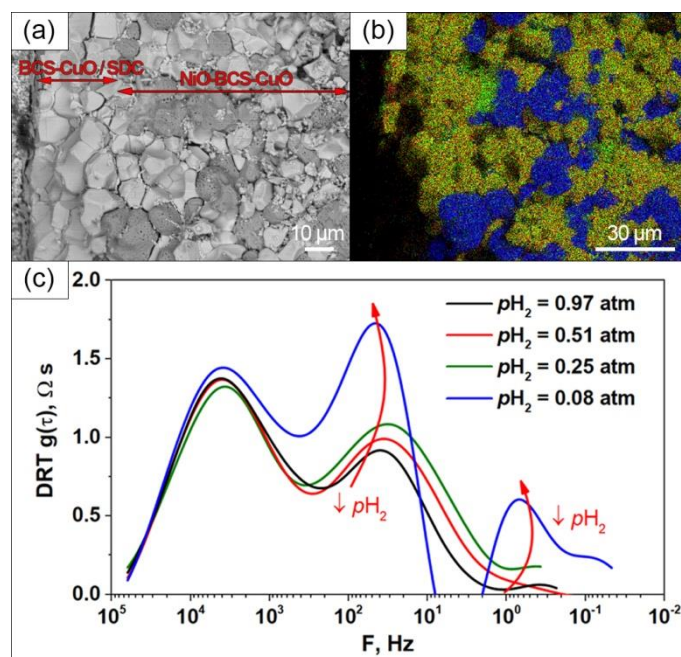


Figure 11 Fracture images of the cell with the BCS–CuO/SDC electrolyte layer on the NiO–BCS–CuO anode substrate sintered at a temperature of 1450 °C after electrochemical testing in the SOFC mode: (a) SEM image, magnification 1500 \times ; (b) integral map of the elements' distribution; (c) frequency dependences of the distribution function of relaxation times of the electrode response for the BCS–SDC cell at various partial pressures of hydrogen in the anode channel at 700 °C. The pick on the left is related to the cathode resistance, on the right – to the supporting anode resistance.

conclude that further development of air electrodes compatible with $\text{CeO}_2/\text{BaCeO}_3$ composite electrolytes is necessary to enhance performance related SOFCs.

A separate direction can be singled out related to the development of the design of SOFCs based on SDC solid electrolyte carrier substrates. The advantage of this SOFC scheme with a carrier electrolyte is the reliable separation of gas channels using a dense electrolyte membrane of sufficient thickness (several hundred microns), this SOFC design has mechanical strength under application conditions. To solve the problem of internal shorting of the MIEC SDC electrolyte, an approach using barrier layers on the anode and cathode sides of the electrolyte membrane can be used [11].

One of the problems of forming barrier layers is to ensure their compatibility with the main electrolyte layer during sintering of the SOFC multilayer structure. For example, the use of unipolar ionic conductors of zirconium dioxide doped with yttria Y_2O_3 (YSZ) as a barrier layer material on an SDC electrolyte encounters significant difficulties associated with delamination and cracking of the coatings [181]. Proton-conducting electrolyte materials based on BaCeO_3 , in particular BCS, are well compatible with the SDC electrolyte material,

which allows it to be used as barrier layers. In this approach was studied by Kalinina&Pikalova group in detail [83]. EPD of $\text{BaCe}_{0.8}\text{Sm}_{0.19}\text{Cu}_{0.1}\text{O}_3$ (BCSCuO) barrier layers was carried out on SDC supporting electrolyte substrates with a thickness of 550 μm . The surface conductivity of the surface of the SDC substrates was ensured by applying conductive sublayers: 1) deposition of a layer of finely dispersed platinum and 2) synthesis of a conductive polymer – polypyrrole. The BCSCuO layers were deposited on an anode or both anode and cathode side on the SDC-based cell and sintered at a temperature of 1530 $^{\circ}\text{C}$ for 5 h. After sintering, dense BCSCuO barrier layers free of cracks and pores were formed on the fabricated samples. In contrast to deposition of bilayer BCS–SDC electrolytes, there was no interdiffusion between the dense SDC substrate and the BCSCuO films. Despite of numerous studies of protonic-based suspensions, the testing the deposited electrolytes in a SOFC mode is poorly represented. We summarized the available literature data in Table 4.

Table 4 – Performance characteristics of IT-SOFCs with proton-conducting electrolyte layers formed by EPD on porous electrode and dense electrolyte substrates.

Substrate (T_{sinty} $^{\circ}\text{C}$)	Electrolyte (T_{sinty} $^{\circ}\text{C}$)	OCV (V)/MPD (W/cm^2) $T(^{\circ}\text{C})$	Refs
NiO- BCY10 + graphite green	BCY10 9.5 μm 1550	1.05/0.296/700 1.07/0.275/650 1.10/0.242/600	[176]
NiO- BCY20 + graphite green	BCY20 9.2 1450 μm	0.94/0.074/600	[75]
NiO-BCS disks, d = 15 mm 1200	BCS_CuO 18 μm SDC 10 μm 1450	0.92/0.070/750 0.050/700	[115]
NiO-BCS disks, 15 mm 1200	BCS_CuO 13 μm SDC 18 μm 1450	0.90/0.160/750 0.080/700 1.05/0.050/650	[115]
SDC h = 550 μm 1600	BCSCuO 18 μm (anode side) 1500	0.809/0.375/800 0.872/0.259/700 0.923/0.141/600	[83]

Conclusions

In this review, we summarized the main trends and most important achievements in the field of electrophoretic formation of SOFC electrolyte layers. The general principles of EPD were briefly presented, including a discussion of the key parameter of suspension stability - the zeta potential, stabilization factors for

suspensions of micro- and nanopowders, and various EPD mechanisms. Works on the EPD of coatings of the traditional YSZ solid electrolyte, as well as works related to the deposition of coatings based on various oxygen-ion, proton-conducting, multilayer and composite electrolytes for intermediate-temperature SOFCs were considered, the results on SOFC testing were summarized in the separate Tables. The main advantages and possibilities of the electrophoretic formation of SOFC electrolyte layers and the limitations inherent to the EPD were discussed. The EPD method was demonstrated to be used in the implementation of the complete technological cycle for the manufacture of SOFC cells, including high-temperature co-sintering. The problem of obtaining dense solid electrolyte layers was shown to be associated with a consistent choice of materials and porosity of the substrates, the choice of the optimal thickness of the solid electrolyte layer and the deposition and sintering modes.

Supplementary materials

No supplementary materials are available.

Funding

This research had no external funding.

Acknowledgements

None.

Author contributions

Elena Pikalova: Project administration; Writing – review & editing.

Elena Kalinina: Project administration; Conceptualization; Writing – original draft.

Nadezhda Pikalova: Visualization; Data curation; Writing – original draft.

Conflict of interest

The authors declare no conflict of interest.

Additional information

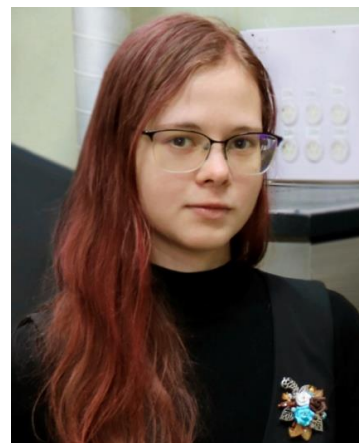


Elena Pikalova, Ph. D, senior researcher of the Laboratory of Solid Oxide Fuel Cells, IHTE UB RAS (Yekaterinburg, Russia), the leader of the group on the development of cathode materials for SOFCs (IHTE UB RAS) and the head researcher in the group of Engineering and economic interdisciplinary research in energy and high-tech industries at the Department of Environmental Economics, Graduate School of Economics and Management, Ural Federal University. She is the author of 104 research papers, h-index 24 (Researcher ID: L-6877-2017; Scopus Author ID: 16242376500; <https://orcid.org/0000-0001-8176-9417>), 9 patents and 3 book chapters and one monograph. Area of scientific interests and research: alternative energy sources, SOFCs, solid state electrolytes, thin-film technologies, cathode materials, MIEC membranes, SOFC interconnects, protective and barrier layers, impedance spectroscopy.



Elena G. Kalinina, Ph. D, Senior researcher of the Complex Electrophysic Investigations Laboratory, IEP UB RAS (Yekaterinburg, Russia), the leader of the group on the development of electrophoretic deposition of thin films in SOFC technology (IEP UB RAS) and Assistant Professor Researcher, Department of Physical and

Inorganic Chemistry, Institute of Natural Sciences and Mathematics (Ural Federal University). She is the author of 45 research papers, h-index 13 (Researcher ID: F-1587-2017; Scopus Author ID: 36697946700; <https://orcid.org/0000-0002-5637-7451>), 8 Patents. Area of scientific interests: electrophoretic deposition (EPD), colloidal systems, thin films, deposition kinetics, ceramic technology, solid oxide fuel cells (SOFCs).



Nadezhda Pikalova, Junior researcher of the High Entropy Alloys Laboratory, IMET UB RAS (Yekaterinburg, Russia). At the moment, she is studying for a master's degree in "Nanoengineering" at the Department of Physical methods and quality control devices, Ural Federal University. She is the author of 6 research papers (Scopus Author ID: 57210390662), h-index: 3. Area of scientific interests and research: cathode materials, solid oxide fuel cells (SOFCs), high entropy alloys (HEAs), nanomaterials, machine learning.

References

1. Mendonça C, Ferreira A, Santos DMF, Towards the Commercialization of Solid Oxide Fuel Cells: Recent Advances in Materials and Integration Strategies, *Fuels*. **2** (2021) 393–419. <https://doi.org/10.3390/fuels2040023>
2. Fallah Vostakola M, Amini Horri B, Progress in Material Development for Low-Temperature Solid Oxide Fuel Cells: A Review, *Energies*. **14** (2021) 1280. <https://doi.org/10.3390/en14051280>
3. Gao Z, Mogni LV, Miller EC, Railsback JG, Barnett SA, A perspective on low-temperature solid oxide fuel cells, *Energy Environ. Sci.* **9** (2016) 1602–1644. <https://doi.org/10.1039/C5EE03858H>
4. da Silva FS, de Souza TM, Novel Materials for Solid Oxide Fuel Cell Technologies: A Literature Review, *Int. J. Hydrog. Energy*. **42** (2017) 26020–26036. <https://doi.org/10.1016/j.ijhydene.2017.08.105>
5. Corigliano O, Pagnotta L, Fragiaco P, On the Technology of Solid Oxide Fuel Cell (SOFC) Energy Systems for Stationary Power Generation: A Review, *Sustainability*. **14** (2022) 15276. <https://doi.org/10.3390/su142215276>
6. Naeini M, Cotton JS, Adams TA, Economically Optimal Sizing and Operation Strategy for Solid Oxide Fuel Cells to Effectively Manage Long-Term Degradation, *Ind. Eng. Chem.*

- Res. **60** (2021) 17128–17142. <https://doi.org/10.1021/acs.iecr.1c03146>
7. Ni M, New developments and challenges of solid oxide fuel cell (SOFC)-based technologies, *Int. J. Energy Res.* **42** (2018) 4526–4531. <https://doi.org/10.1002/er.4213>
8. Zhigachev AO, Rodaev VV, Zhigacheva DV, Lyskov NV, Shchukina MA, Doping of scandia-stabilized zirconia electrolytes for intermediate-temperature solid oxide fuel cell: A review, *Ceram. Int.* **47** (2021) 32490–32504. <https://doi.org/10.1016/j.ceramint.2021.08.285>
9. Filonova E, Medvedev D, Recent Progress in the Design, Characterisation and Application of LaAlO₃- and LaGaO₃-Based Solid Oxide Fuel Cell Electrolytes, *Nanomater.* **12** (2022) 1991. <https://doi.org/10.3390/nano12121991>
10. Morales M, Roa JJ, Tartaj J, Segarra M, A review of doped lanthanum gallates as electrolytes for intermediate temperature solid oxides fuel cells: From materials processing to electrical and thermo-mechanical properties, *J. Eur. Ceram. Soc.* **36** (2016) 1–16. <https://doi.org/10.1016/j.jeurceramsoc.2015.09.025>
11. Pikalova EYu, Kalinina EG, Solid oxide fuel cells based on ceramic membranes with mixed conductivity: improving efficiency, *Russ. Chem. Rev.* **90** (2021) 703–749. <https://doi.org/10.1070/RCR4966>
12. Jaiswal N, Tanwar K, Suman R, Kumar D, Upadhyay S, Parkash O, A brief review on ceria based solid electrolytes for solid oxide fuel cells, *J. Alloys Compd.* **781** (2019) 984–1005. <https://doi.org/10.1016/j.jallcom.2018.12.015>
13. Pikalova EYu, Ermakova LV, Vlasov MI, Fluorine doping as a feasible method to enhancing functional properties of Ce_{0.8}Sm_{0.2}O_{1.9} electrolyte, *Int. J. Hydrog. Energy.* (2023) In Press. <https://doi.org/10.1016/j.ijhydene.2022.11.238>
14. Tarasova NA, Animitsa IE, Galisheva AO, Medvedev DA, Layered and hexagonal perovskites as novel classes of proton-conducting solid electrolytes. A focus review, *Electrochem. Mater. Technol.* **1** (2022) 20221004. <https://doi.org/10.15826/elmattech.2022.1.004>
15. Medvedev DA, Lyagaeva JG, Gorbova EV, Demin AK, Tsiakaras P, Advanced materials for SOFC application: Strategies for the development of highly conductive and stable solid oxide proton electrolytes, *Prog. Mater. Sci.* **75** (2016) 38–79. <https://doi.org/10.1016/j.pmatsci.2015.08.001>
16. Zhang W, Hu YH, Progress in proton-conducting oxides as electrolytes for low-temperature solid oxide fuel cells: From materials to devices, *Energy Sci. Eng.* **9** (2021) 984–1011. <https://doi.org/10.1002/ese3.886>
17. Zhang J, Ricote S, Hendriksen PV, Chen Y, Advanced Materials for Thin-Film Solid Oxide Fuel Cells: Recent Progress and Challenges in Boosting the Device Performance at Low Temperatures, *Adv. Funct. Mater.* **32** (2022) 2111205. <https://doi.org/10.1002/adfm.202111205>
18. Tucker MC, Progress in metal-supported solid oxide fuel cells: A review, *J. Power Sources.* **195** (2010) 4570–4582. <https://doi.org/10.1016/j.jpowsour.2010.02.035>
19. Agarkova EA, Burmistrov IN, Agarkov DA, Zadorozhnaya OYu, Shipilova AV, Solovyev AA, et al., Bilayered anode supports for planar solid oxide fuel cells: Fabrication and electrochemical performance, *Mater. Lett.* **283** (2021) 128752. <https://doi.org/10.1016/j.matlet.2020.128752>
20. Dunyushkina LA, Solid Oxide Fuel Cells with a Thin Film Electrolyte: A Review on Manufacturing Technologies and Electrochemical Characteristics, *Electrochem. Mater. Technol.* **1** (2022) 20221006. <https://doi.org/10.15826/elmattech.2022.1.006>
21. Besra L, Liu M, A review on fundamentals and applications of electrophoretic deposition (EPD), *Prog. Mater. Sci.* **52** (2007) 1–61. <https://doi.org/10.1016/j.pmatsci.2006.07.001>
22. Corni I, Ryan MP, Boccacini AR, Electrophoretic deposition: From traditional ceramics to nanotechnology, *J. Eur. Ceram. Soc.* **28** (2008) 1353–1367. <https://doi.org/10.1016/j.jeurceramsoc.2007.12.011>
23. Lee SH, Woo SP, Kakati N, Kim D-J, Yoon YS, A Comprehensive Review of Nanomaterials Developed Using Electrophoresis Process for High-Efficiency Energy Conversion and Storage Systems, *Energies.* **11** (2018) 3122. <https://doi.org/10.3390/en11113122>
24. Aznam I, Mah JWC, Muchtar A, Somalu MR, Ghazali MJ, A review of key parameters for effective electrophoretic deposition in the fabrication of solid oxide fuel cells, *J. Zhejiang Univ.-Sci. A.* **19** (2018) 811–823. <https://doi.org/10.1631/jzus.A1700604>
25. Kalinina EG, Pikalova EYu, New trends in the development of electrophoretic deposition method in the solid oxide fuel cell technology: theoretical approaches, experimental solutions and development prospects, *Russ. Chem. Rev.* **88** (2019) 1179–1219. <https://doi.org/10.1070/RCR4889>
26. Pikalova EYu, Kalinina EG, Electrophoretic deposition in the solid oxide fuel cell technology: Fundamentals and recent advances, *Renew. Sustain. Energy Rev.* **116** (2019) 109440. <https://doi.org/10.1016/j.rser.2019.109440>
27. Pikalova EYu, Kalinina EG, Place of electrophoretic deposition among thin-film methods adapted to the solid oxide fuel cell technology: A short review, *Int. J. Energy Prod. Manag.* **4** (2019) 1–27. <https://doi.org/10.2495/EQ-V4-N1-I-27>
28. Kalinina E, Pikalova E, Opportunities, Challenges and Prospects for Electrodeposition of Thin-Film Functional Layers in Solid Oxide Fuel Cell Technology, *Materials.* **14** (2021) 5584. <https://doi.org/10.3390/ma14195584>
29. Solovev AV, Starostin GN, Zvonareva IA, Tulenin SS, Markov VF, Electrophoretic deposition of YSZ layers on pyrolytic graphite and a porous anode substrate based on NiO-YSZ, *Chim. Techno Acta.* **9** (2022) 20229425, 6321. <https://doi.org/10.15826/chimtech.2022.9.4.25>
30. Van der Biest OO, Vandeperre LJ, Electrophoretic deposition of materials, *Annu. Rev. Mater. Sci.* **29** (1999) 327–352. <https://doi.org/10.1146/annurev.matsci.29.1.327>
31. The cataphoresis of suspended particles. Part I.—The equation of cataphoresis, *Proc. R. Soc. Lond. Ser. Contain. Pap. Math. Phys. Character.* **133** (1931) 106–129. <https://doi.org/10.1098/rspa.1931.0133>
32. Sarkar P, Nicholson PS, Electrophoretic Deposition (EPD): Mechanisms, Kinetics, and Application to Ceramics, *J. Am. Ceram. Soc.* **79** (1996) 1987–2002. <https://doi.org/10.1111/j.1151-2916.1996.tb08929.x>
33. Hunter RJ Zeta Potential in Colloid Science, Elsevier, 1981: p. 386. <https://doi.org/10.1016/B978-0-12-361961-7.50001-8>
34. Serrano-Lotina A, Portela R, Baeza P, Alcolea-Rodriguez V, Villarroya M, Ávila P, Zeta potential as a tool for functional materials development, *Catal. Today.* (2022) In Press. <https://doi.org/10.1016/j.cattod.2022.08.004>

35. Jailani S, Franks GV, Healy TW, ζ Potential of Nanoparticle Suspensions: Effect of Electrolyte Concentration, Particle Size, and Volume Fraction, *J. Am. Ceram. Soc.* **91** (2008) 1141–1147. <https://doi.org/10.1111/j.1551-2916.2008.02277.x>
36. Carrique F, Arroyo FJ, Jiménez ML, Delgado AV, Influence of Double-Layer Overlap on the Electrophoretic Mobility and DC Conductivity of a Concentrated Suspension of Spherical Particles, *J. Phys. Chem. B.* **107** (2003) 3199–3206. <https://doi.org/10.1021/jp027148k>
37. Kalinina EG, Electrokinetic Properties of Nanopowder Suspensions Based on Aluminum Oxide, Obtained via the Electric Explosion of a Wire, *Russ. J. Phys. Chem. A.* **96** (2022) 2032–2037. <https://doi.org/10.1134/S0036024422090163>
38. Zhitomirsky I, Cathodic electrodeposition of ceramic and organoceramic materials. Fundamental aspects, *Adv. Colloid Interface Sci.* **97** (2002) 279–317. [https://doi.org/10.1016/S0001-8686\(01\)00068-9](https://doi.org/10.1016/S0001-8686(01)00068-9)
39. Bhattacharjee S, DLS and zeta potential – What they are and what they are not? *J. Control. Release.* **235** (2016) 337–351. <https://doi.org/10.1016/j.jconrel.2016.06.017>
40. Will J, Hruschka MKM, Gubler L, Gauckler LJ, Electrophoretic Deposition of Zirconia on Porous Anodic Substrates, *J. Am. Ceram. Soc.* **84** (2004) 328–32. <https://doi.org/10.1111/j.1151-2916.2001.tb00658.x>
41. Sora I, Pelosato R, Simone A, Montanaro L, Maglia F, Chioldelli G, Characterization of LSGM films obtained by electrophoretic deposition (EPD), *Solid State Ion.* **177** (2006) 1985–1989. <https://doi.org/10.1016/j.ssi.2006.03.022>
42. Kalinina EG, Safronov AP, Kotov YuA, Formation of thin YSZ electrolyte films by electrophoretic deposition on porous cathodes, *Russ. J. Electrochem.* **47** (2011) 671–675. <https://doi.org/10.1134/S1023193511060036>
43. Krkljuš I, Branković Z, Đuriš K, Vukotić V, Branković G, Bernik S, The Electrophoretic Deposition of Lanthanum Manganite Powders for a Cathode-Supported Solid Oxide Fuel Cell in Planar and Tubular Configurations, *Int. J. Appl. Ceram. Technol.* **5** (2008) 548–556. <https://doi.org/10.1111/j.1744-7402.2008.02218.x>
44. Kalinina EG, Efimov AA, Safronov AP, The influence of nanoparticle aggregation on formation of ZrO₂ electrolyte thin films by electrophoretic deposition, *Thin Solid Films.* **612** (2016) 66–71. <https://doi.org/10.1016/j.tsf.2016.05.039>
45. Kalinina E, Pikalova E, Ermakova L, Bogdanovich N, Challenges of Formation of Thin-Film Solid Electrolyte Layers on Non-Conductive Substrates by Electrophoretic Deposition, *Coatings.* **11** (2021) 805. <https://doi.org/10.3390/coatings11070805>
46. Saji VS, Electrophoretic-deposited Superhydrophobic Coatings, *Chem. – Asian J.* **16** (2021) 474–491. <https://doi.org/10.1002/asia.202001425>
47. Kalinina EG, Pikalova EYu, Menshikova AV, Nikolaenko IV, Electrophoretic deposition of a self-stabilizing suspension based on a nanosized multi-component electrolyte powder prepared by the laser evaporation method, *Solid State Ion.* **288** (2016) 110–114. <https://doi.org/10.1016/j.ssi.2015.12.008>
48. Metzger C, Drexel R, Meier F, Briesen H, Effect of ultrasonication on the size distribution and stability of cellulose nanocrystals in suspension: an asymmetrical flow field-flow fractionation study, *Cellulose.* **28** (2021) 10221–10238. <https://doi.org/10.1007/s10570-021-04172-3>
49. Negishi H, Yamaji K, Sakai N, Horita T, Yanagishita H, Yokokawa H, Electrophoretic deposition of YSZ powders for solid oxide fuel cells, *J. Mater. Sci.* **39** (2004) 833–838. <https://doi.org/10.1023/B:JMASC.0000012911.86185.13>
50. Panigrahi S, Bhattacharjee S, Besra L, Singh BP, Sinha SP, Electrophoretic deposition of doped ceria: Effect of solvents on deposition microstructure, *J. Eur. Ceram. Soc.* **30** (2010) 1097–1103. <https://doi.org/10.1016/j.jeurceramsoc.2009.06.038>
51. Chauoon S, Meepho M, Chuankrerkkul N, Chaianansutcharit S, Pornprasertsuk R, Fabrication of yttria stabilized zirconia thin films on powder-injected anode substrates by electrophoretic deposition technique for solid oxide fuel cell application, *Thin Solid Films.* **660** (2018) 741–748. <https://doi.org/10.1016/j.tsf.2018.03.082>
52. Oskouyi OE, Shahmiri M, Maghsoudipour A, Hasheminasari M, Pulsed constant voltage electrophoretic deposition of YSZ electrolyte coating on conducting porous Ni-YSZ cermet for SOFCs applications, *J. Alloys Compd.* **785** (2019) 220–227. <https://doi.org/10.1016/j.jallcom.2019.01.166>
53. Zhitomirsky I, Petric A, Electrophoretic deposition of ceramic materials for fuel cell applications, *J. Eur. Ceram. Soc.* **20** (2000) 2055–2061. [https://doi.org/10.1016/S0955-2219\(00\)00098-4](https://doi.org/10.1016/S0955-2219(00)00098-4)
54. Das D, Basu RN, Organic acids as electrostatic dispersing agents to prepare high quality particulate thin film, *J. Alloys Compd.* **729** (2017) 71–83. <https://doi.org/10.1016/j.jallcom.2017.09.097>
55. Das D, Bagchi B, Basu RN, Nanostructured zirconia thin film fabricated by electrophoretic deposition technique, *J. Alloys Compd.* **693** (2017) 1220–1230. <https://doi.org/10.1016/j.jallcom.2016.10.088>
56. Xu Z, Rajaram G, Sankar J, Pai D, Electrophoretic deposition of YSZ electrolyte coatings for SOFCs, *Fuel Cells Bull.* **2007** (2007) 12–16. [https://doi.org/10.1016/S1464-2859\(07\)70114-1](https://doi.org/10.1016/S1464-2859(07)70114-1)
57. Pantoja-Pertega J, Díaz-Parralejo A, Macías-García A, Sánchez-González J, Cuerda-Correa EM, Design, preparation, and characterization of Yttria-Stabilized Zirconia (YSZ) coatings obtained by electrophoretic deposition (EPD), *Ceram. Int.* **47** (2021) 13312–13321. <https://doi.org/10.1016/j.ceramint.2020.12.279>
58. Kherad R, Dodangei S, Moussavi SH, Ghatee M, Characterization of anode supported micro-tubular solid oxide fuel cells prepared by successive non-aqueous electrophoretic deposition, *J. Electroceram.* **48** (2022) 1–7. <https://doi.org/10.1007/s10832-021-00272-5>
59. Yamaji K, Kishimoto H, Xiong Y, Horita T, Sakai N, Performance of anode-supported SOFCs fabricated with electrophoretic deposition techniques, *Fuel Cells Bull.* **2004** (2004) 12–15. [https://doi.org/10.1016/S1464-2859\(04\)00445-6](https://doi.org/10.1016/S1464-2859(04)00445-6)
60. Hu S, Li W, Yao M, Li T, Liu X, Electrophoretic Deposition of Gadolinium-doped Ceria as a Barrier Layer on Yttrium-stabilized Zirconia Electrolyte for Solid Oxide Fuel Cells, *Fuel Cells.* **17** (2017) 869–874. <https://doi.org/10.1002/fuce.201700122>
61. Hu S, Li W, Li W, Zhang N, Qi H, Finklea H, Liu X, A study on the electrophoretic deposition of gadolinium doped ceria on polypyrrole coated yttrium stabilized zirconia, *J. Colloid Interface Sci.* **555** (2019) 115–123. <https://doi.org/10.1016/j.jcis.2019.07.094>

62. Ichiboshi H, Myoujin K, Kodera T, Ogihara T, Preparation of $\text{Ce}_{0.8}\text{Sm}_{0.2}\text{O}_{1.9}$ Thin Films by Electrophoretic Deposition and their Fuel Cell Performance, *Key Eng. Mater.* **566** (2013) 137–140. <https://doi.org/10.4028/www.scientific.net/KEM.566.137>
63. Suarez G, Nguyen NTK, Rendtorff NM, Sakka Y, Uchikoshi T, Electrophoretic deposition for obtaining dense lanthanum silicate oxyapatite (LSO), *Ceram. Int.* **42** (2016) 19283–19288. <https://doi.org/10.1016/j.ceramint.2016.09.095>
64. Jothinathan E, Biest OV der, Vleugels J, Electrophoretic deposition of apatite type lanthanum silicates for SOFC half-cell production, *Adv. Appl. Ceram.* **111** (2012) 459–465. <https://doi.org/10.1179/1743676112Y.0000000015>
65. Argiris C, Grosse-Brauckmann J, Sourkouni G, Taillades G, Roziere J, Preparation of Thin Proton Conducting Membranes by Means of EPD, *Key Eng. Mater.* **412** (2009) 125–130. <https://doi.org/10.4028/www.scientific.net/KEM.412.125>
66. Choudhary B, Anwar S, Besra L, Anwar S, Electrophoretic deposition studies of $\text{Ba}(\text{Zr-Ce-Y})\text{O}_3$ ceramic coating, *Int. J. Appl. Ceram. Technol.* **16** (2019) 1022–1031. <https://doi.org/10.1111/ijac.13152>
67. Ishihara T, Sato K, Takita Y, Electrophoretic Deposition of Y_2O_3 -Stabilized ZrO_2 Electrolyte Films in Solid Oxide Fuel Cells, *J. Am. Ceram. Soc.* **79** (1996) 913–919. <https://doi.org/10.1111/j.1151-2916.1996.tb08525.x>
68. Majhi SM, Behura SK, Bhattacharjee S, Singh BP, Chongdar TK, Gokhale NM, L. Besra L, Anode supported solid oxide fuel cells (SOFC) by electrophoretic deposition, *Int. J. Hydrog. Energy.* **36** (2011) 14930–14935. <https://doi.org/10.1016/j.ijhydene.2011.02.100>
69. Kalinina EG, Lyutyagina NA, Leiman DV, Safronov AP, Influence of the degree of deaggregation of YSZ nanopowders in suspension on the process of electrophoretic deposition, *Nanotechnologies Russ.* **9** (2014) 274–279. <https://doi.org/10.1134/S1995078014030069>
70. Salehzadeh D, Torabi M, Sadeghian Z, Marashi P, A multiscale-architecture solid oxide fuel cell fabricated by electrophoretic deposition technique, *J. Alloys Compd.* **830** (2020) 154654. <https://doi.org/10.1016/j.jallcom.2020.154654>
71. Kobayashi K, Supported $\text{Zr}(\text{Sc})\text{O}_2$ SOFCs for reduced temperature prepared by electrophoretic deposition, *Solid State Ion.* **152–153** (2002) 591–596. [https://doi.org/10.1016/S0167-2738\(02\)00392-2](https://doi.org/10.1016/S0167-2738(02)00392-2)
72. Nakayama S, Miyayama M, Fabrication and Fuel-Cell Properties of Sm-Doped CeO_2 Electrolyte Film by Electrophoretic Deposition, *Key Eng. Mater.* **350** (2007) 175–178. <https://doi.org/10.4028/www.scientific.net/KEM.350.175>
73. Ou DR, Mori T, Ye F, Miyayama M, Nakayama S, Zou J, et al., Microstructural Characteristics of SDC Electrolyte Film Supported by Ni-SDC Cermet Anode, *J. Electrochem. Soc.* **156** (2009) B825. <https://doi.org/10.1149/1.3129436>
74. Di Bartolomeo E, Zunic M, Chevallier L, D'Epifanio A, Licocchia S, Traversa E, Fabrication of Proton Conducting Solid Oxide Fuel Cells by using Electrophoretic Deposition, *ECS Trans.* **25** (2009) 577–584. <https://doi.org/10.1149/1.3205569>
75. Itagaki Y, Yamamoto Y, Aono H, Yahiro H, Anode-supported SOFC with thin film of proton-conducting $\text{BaCe}_{0.8}\text{Y}_{0.2}\text{O}_{3-6}$ by electrophoretic deposition, *J. Ceram. Soc. Jpn.* **125** (2017) 528–532. <https://doi.org/10.2109/jcersj2.17048>
76. Chen F, Liu M, Preparation of yttria-stabilized zirconia (YSZ) films on $\text{La}_{0.85}\text{Sr}_{0.15}\text{MnO}_3$ (LSM) and LSM-YSZ substrates using an electrophoretic deposition (EPD) process, *J. Eur. Ceram. Soc.* **21** (2001) 127–134. [https://doi.org/10.1016/S0955-2219\(00\)00195-3](https://doi.org/10.1016/S0955-2219(00)00195-3)
77. Kalinina EG, Pikalova EYu, Preparation and Properties of Stable Suspensions of ZrO_2 - Y_2O_3 Powders with Different Particle Sizes for Electrophoretic Deposition, *Inorg. Mater.* **56** (2020) 941–948. <https://doi.org/10.1134/S0020168520090095>
78. Kalinina EG, Samatov OM, Safronov AP, Stable suspensions of doped ceria nanopowders for electrophoretic deposition of coatings for solid oxide fuel cells, *Inorg. Mater.* **52** (2016) 858–864. <https://doi.org/10.1134/S0020168516080094>
79. Kalinina EG, Pikalova EYu, Kolchugin AA, Pikalov SM, Kaigorodov AS, Cyclic electrophoretic deposition of electrolyte thin-films on the porous cathode substrate utilizing stable suspensions of nanopowders, *Solid State Ion.* **302** (2017) 126–132. <https://doi.org/10.1016/j.ssi.2017.01.016>
80. Kalinina EG, Bogdanovich NM, Bronin DI, Pikalova EYu, Pankratov AA, Formation of Thin-Film Electrolyte by Electrophoretic Deposition onto Modified Multilayer Cathode, *Russ. J. Appl. Chem.* **92** (2019) 191–198. <https://doi.org/10.1134/S1070427219020046>
81. Kalinina E, Pikalova E, Kolchugin A, Pikalova N, Farlenkov A, Comparative Study of Electrophoretic Deposition of Doped BaCeO_3 -Based Films on $\text{La}_2\text{NiO}_{4+6}$ and $\text{La}_{1.7}\text{Ba}_{0.3}\text{NiO}_{4+6}$ Cathode Substrates, *Materials.* **12** (2019) 2545. <https://doi.org/10.3390/ma12162545>
82. Kalinina E, Kolchugin A, Shubin K, Farlenkov A, Pikalova E, Features of Electrophoretic Deposition of a Ba-Containing Thin-Film Proton-Conducting Electrolyte on a Porous Cathode Substrate, *Appl. Sci.* **10** (2020) 6535. <https://doi.org/10.3390/app10186535>
83. Kalinina E, Shubin K, Pikalova E, Electrophoretic Deposition and Characterization of the Doped BaCeO_3 Barrier Layers on a Supporting $\text{Ce}_{0.8}\text{Sm}_{0.2}\text{O}_{1.9}$ Solid-State Electrolyte, *Membranes.* **12** (2022) 308. <https://doi.org/10.3390/membranes12030308>
84. Kalinina EG, Pikalova EYu, Modifying Suspensions for the Electrophoretic Deposition of $\text{BaCe}_{0.5}\text{Zr}_{0.3}\text{Y}_{0.1}\text{Yb}_{0.1}\text{O}_{3-6}$ Solid Electrolyte, *Russ. J. Phys. Chem. A.* **95** (2021) 1942–1947. <https://doi.org/10.1134/S0036024421090077>
85. Cherng JS, Sau JR, Chung CC, Aqueous electrophoretic deposition of YSZ electrolyte layers for solid oxide fuel cells, *J. Solid State Electrochem.* **12** (2008) 925–933. <https://doi.org/10.1007/s10008-007-0458-2>
86. Cherng JS, Wu CC, Chen WH, Yeh TH, Microstructure and performance of micro-tubular solid oxide fuel cells made by aqueous electrophoretic deposition, *Ceram. Int.* **39** (2013) S601–S604. <https://doi.org/10.1016/j.ceramint.2012.10.144>
87. Hu S, Li W, Li W, Zhang N, Qi H, Finklea H, Liu X, Aqueous electrophoretic deposition of gadolinium doped ceria, *Colloids Surf. Physicochem. Eng. Asp.* **579** (2019) 123717. <https://doi.org/10.1016/j.colsurfa.2019.123717>
88. Yamamoto K, Sato K, Matsuda M, Ozawa M, Ohara S, Anomalous low-temperature sintering of a solid electrolyte thin film of tailor-made nanocrystals on a porous cathode support for low-temperature solid oxide fuel cells, *Ceram. Int.* **47** (2021) 15939–15946. <https://doi.org/10.1016/j.ceramint.2021.02.168>
89. Oskouyi OE, Maghsoudipour A, Shahmiri M, Hasheminasari M, Preparation of YSZ electrolyte coating on conducting porous Ni-YSZ cermet by DC and pulsed constant voltage electrophoretic deposition process for SOFCs

applications, *J. Alloys Compd.* **795** (2019) 361–369.

<https://doi.org/10.1016/j.jallcom.2019.04.334>

90. Talebi T, Raissi B, Maghsoudipour A, The role of addition of water to non-aqueous suspensions in electrophoretically deposited YSZ films for SOFCs, *Int. J. Hydrog. Energy.* **35** (2010) 9434–9439.

<https://doi.org/10.1016/j.ijhydene.2009.12.152>

91. Das D, Basu RN, Suspension chemistry and electrophoretic deposition of zirconia electrolyte on conducting and non-conducting substrates, *Mater. Res. Bull.* **48** (2013) 3254–3261.

<https://doi.org/10.1016/j.materresbull.2013.05.034>

92. Kalinina EG, Rusakova DS, Pikalova EYu, Peculiarities of electrophoretic deposition and morphology of deposited films in non-aqueous suspensions of Al₂O₃-Al nanopowder, *Chim. Techno Acta.* **9** (2022) 20229207, 5881.

<https://doi.org/10.15826/chimtech.2022.9.2.07>

93. Guo F, Shapiro IP, Xiao P, Effect of HCl on electrophoretic deposition of yttria stabilized zirconia particles in organic solvents, *J. Eur. Ceram. Soc.* **31** (2011) 2505–2511.

<https://doi.org/10.1016/j.jeurceramsoc.2011.02.027>

94. Xu H, Shapiro IP, Xiao P, pH Effect on Electrophoretic Deposition in Non-Aqueous Suspensions and Sintering of YSZ Coatings, *Key Eng. Mater.* **412** (2009) 165–170.

<https://doi.org/10.4028/www.scientific.net/KEM.412.165>

95. Sarkar P, Huang X, Nicholson PS, Zirconia/Alumina Functionally Graded Composites by Electrophoretic Deposition Techniques, *J. Am. Ceram. Soc.* **76** (1993) 1055–1056.

<https://doi.org/10.1111/j.1151-2916.1993.tb05335.x>

96. Hanaor D, Michelazzi M, Leonelli C, Sorrell CC, The effects of carboxylic acids on the aqueous dispersion and electrophoretic deposition of ZrO₂, *J. Eur. Ceram. Soc.* **32** (2012) 235–244.

<https://doi.org/10.1016/j.jeurceramsoc.2011.08.015>

97. Xu H, Shapiro IP, Xiao P, The influence of pH on particle packing in YSZ coatings electrophoretically deposited from a non-aqueous suspension, *J. Eur. Ceram. Soc.* **30** (2010) 1105–1114.

<https://doi.org/10.1016/j.jeurceramsoc.2009.07.021>

98. Ahmadi M, Aghajani H, Suspension characterization and electrophoretic deposition of Yttria-stabilized Zirconia nanoparticles on an iron-nickel based superalloy, *Ceram. Int.* **43** (2017) 7321–7328.

<https://doi.org/10.1016/j.ceramint.2017.03.035>

99. Olevsky EA, Wang X, Maximenko A, Meyers MA, Fabrication of Net-Shape Functionally Graded Composites by Electrophoretic Deposition and Sintering: Modeling and Experimentation, *J. Am. Ceram. Soc.* **90** (2007) 3047–3056.

<https://doi.org/10.1111/j.1551-2916.2007.01838.x>

100. Zarbov M, Schuster I, Gal-Or L, Methodology for selection of charging agents for electrophoretic deposition of ceramic particles, *J. Mater. Sci.* **39** (2004) 813–817.

<https://doi.org/10.1023/B:JMASC.0000012908.18329.93>

101. Kotov YuA, Electric Explosion of Wires as a Method for Preparation of Nanopowders, *J. Nanoparticle Res.* **5** (2003) 539–550.

<https://doi.org/10.1023/B:NANO.0000006069.45073.0b>

102. Kotov YuA, The electrical explosion of wire: A method for the synthesis of weakly aggregated nanopowders, *Nanotechnol. Russ.* **4** (2009) 415–424.

<https://doi.org/10.1134/S1995078009070039>

103. Ivanov M, Osipov V, Kotov Yu, Lisenkov V, Platonov V, Solomonov V, Laser Synthesis of Oxide Nanopowders, *Adv. Sci. Technol.* **45** (2006) 291–296.

<https://doi.org/10.4028/www.scientific.net/AST.45.291>

104. Kalinina EG, Pikalova EYu, Safronov AP, A study of the electrophoretic deposition of thin-film coatings based on barium cerate nanopowder produced by laser evaporation, *Russ. J. Appl. Chem.* **90** (2017) 701–707.

<https://doi.org/10.1134/S1070427217050056>

105. Safronov AP, Kalinina EG, Smirnova TA, Leiman DV, Bagazeev AV, Self-stabilization of aqueous suspensions of alumina nanoparticles obtained by electrical explosion, *Russ. J. Phys. Chem. A.* **84** (2010) 2122–2127.

<https://doi.org/10.1134/S0036024410120204>

106. Santillán MJ, Caneiro A, Quaranta N, Boccaccini AR, Electrophoretic deposition of La_{0.6}Sr_{0.4}Co_{0.8}Fe_{0.2}O_{3-δ} cathodes on Ce_{0.9}Gd_{0.1}O_{1.95} substrates for intermediate temperature solid oxide fuel cell (IT-SOFC), *J. Eur. Ceram. Soc.* **29** (2009) 1125–1132.

<https://doi.org/10.1016/j.jeurceramsoc.2008.07.057>

107. Hamaker HC, Verwey EJW, Part II. Colloid stability. The role of the forces between the particles in electrodeposition and other phenomena, *Trans Faraday Soc.* **35** (1940) 180–185.

<https://doi.org/10.1039/TF9403500180>

108. Besra L, Uchikoshi T, Suzuki TS, Sakka Y, Experimental verification of pH localization mechanism of particle consolidation at the electrode/solution interface and its application to pulsed DC electrophoretic deposition (EPD), *J. Eur. Ceram. Soc.* **30** (2010) 1187–1193.

<https://doi.org/10.1016/j.jeurceramsoc.2009.07.004>

109. Grillon F, Fayeulle D, Jeandin M, Quantitative image analysis of electrophoretic coatings, *J. Mater. Sci. Lett.* **11** (1992) 272–275.

<https://doi.org/10.1007/BF00729410>

110. Koelmans H, Overbeek JThG, Stability and electrophoretic deposition of suspensions in non-aqueous media, *Discuss. Faraday Soc.* **18** (1954) 52.

<https://doi.org/10.1039/df9541800052>

111. van der Biest O, Put S, Anné G, Vleugels J, Electrophoretic deposition for coatings and free standing objects, *J. Mater. Sci.* **39** (2004) 779–785.

<https://doi.org/10.1023/B:JMASC.0000012905.62256.39>

112. Ammam M, Electrophoretic deposition under modulated electric fields: a review, *RSC Adv.* **2** (2012) 7633.

<https://doi.org/10.1039/c2ra01342h>

113. Panigrahi S, Besra L, Singh BP, Sinha SP, Bhattacharjee S, Electrophoretic deposition of doped ceria in anti-gravity set-up, *Adv. Powder Technol.* **22** (2011) 570–575.

<https://doi.org/10.1016/j.apt.2010.08.005>

114. Matsuda M, Hosomi T, Murata K, Fukui T, Miyake M, Fabrication of bilayered YSZ/SDC electrolyte film by electrophoretic deposition for reduced-temperature operating anode-supported SOFC, *J. Power Sources.* **165** (2007) 102–107.

<https://doi.org/10.1016/j.jpowsour.2006.11.087>

115. Pikalova E, Osinkin D, Kalinina E, Direct Electrophoretic Deposition and Characterization of Thin-Film Membranes Based on Doped BaCeO₃ and CeO₂ for Anode-Supported Solid Oxide Fuel Cells, *Membranes.* **12** (2022) 682.

<https://doi.org/10.3390/membranes12070682>

116. Talic B, Wulff AC, Molin S, Andersen KB, Zielke P, Frandsen HL, Investigation of electrophoretic deposition as a method for coating complex shaped steel parts in solid oxide cell

- stacks, *Surf. Coat. Technol.* **380** (2019) 125093. <https://doi.org/10.1016/j.surfcoat.2019.125093>
117. Zanchi E, Sabato AG, Molin S, Cempura G, Boccacini AR, Smeacetto F, Recent advances on spinel-based protective coatings for solid oxide cell metallic interconnects produced by electrophoretic deposition, *Mater. Lett.* **286** (2021) 129229. <https://doi.org/10.1016/j.matlet.2020.129229>
118. Matsuda M, Hashimoto M, Matsunaga C, Suzuki TS, Sakka Y, Uchikoshi T, Electrophoretic fabrication of a-b plane oriented La_2NiO_4 cathode onto electrolyte in strong magnetic field for low-temperature operating solid oxide fuel cell, *J. Eur. Ceram. Soc.* **36** (2016) 4077–4082. <https://doi.org/10.1016/j.jeurceramsoc.2016.06.043>
119. Itagaki Y, Yahiro H, Electrophoretic Deposition of Electrode Membrane for Solid Oxide Fuel Cells, ECS Meet. Abstr. **MA2018-01** (2018) 1201–1201. <https://doi.org/10.1149/MA2018-01/18/1201>
120. Zarabian M, Yar AY, Vafaenezhad S, Sani MAF, Simchi A, A. Simchi, Electrophoretic deposition of functionally-graded NiO–YSZ composite films, *J. Eur. Ceram. Soc.* **33** (2013) 1815–1823. <https://doi.org/10.1016/j.jeurceramsoc.2013.01.032>
121. Basu RN, Randall CA, Mayo MJ, Fabrication of Dense Zirconia Electrolyte Films for Tubular Solid Oxide Fuel Cells by Electrophoretic Deposition, *J. Am. Ceram. Soc.* **84** (2001) 33–40. <https://doi.org/10.1111/j.1151-2916.2001.tb00604.x>
122. Fung K-Z, Chen T-Y, Cathode-supported SOFC using a highly conductive lanthanum aluminate-based electrolyte, *Solid State Ion.* **188** (2011) 64–68. <https://doi.org/10.1016/j.ssi.2010.09.035>
123. Yu FA, Wu CC, Yeh TH, Cherng JS, Effects of layer thickness on the performance of micro-tubular solid oxide fuel cells made by sequential aqueous electrophoretic deposition, *Int. J. Hydrog. Energy.* **40** (2015) 14072–14076. <https://doi.org/10.1016/j.ijhydene.2015.05.191>
124. Cherng JS, Ho MY, Yeh TH, Chen WH, Anode-supported micro-tubular SOFCs made by aqueous electrophoretic deposition, *Ceram. Int.* **38** (2012) S477–S480. <https://doi.org/10.1016/j.ceramint.2011.05.057>
125. Ivanov M, Kalinina E, Kopylov Y, Kravchenko V, Krutikova I, Kynast U, Li J, Leznina M, Medvedev A, Highly transparent Yb-doped $(\text{La}_x\text{Y}_{1-x})_2\text{O}_3$ ceramics prepared through colloidal methods of nanoparticles compaction, *J. Eur. Ceram. Soc.* **36** (2016) 4251–4259. <https://doi.org/10.1016/j.jeurceramsoc.2016.06.013>
126. Laska A, Parameters of the electrophoretic deposition process and its influence on the morphology of hydroxyapatite coatings. Review, *Inż. Mater.* **1** (2020) 20–25. <https://doi.org/10.15199/28.2020.1.3>
127. Mochales C, Zehbe R, Frank S, Rahimi F, Urbanska A, Fleck C, Müller WD, Multilayered Ceramic Constructs Created by EPD, *Key Eng. Mater.* **654** (2015) 122–126. <https://doi.org/10.4028/www.scientific.net/KEM.654.122>
128. Lee S-H, Park Y-T, Park J-W, Lee K-T, Fabrication of Symmetrical $\text{La}_{0.7}\text{Ca}_{0.3}\text{Cr}_{0.8}\text{Mn}_{0.2}\text{O}_{3-\delta}$ Electrode Scaffold-Type Micro Tubular Solid Oxide Fuel Cells By Electrophoretic Deposition, ECS Meet. Abstr. **MA2016-02** (2016) 3955–3955. <https://doi.org/10.1149/MA2016-02/53/3955>
129. König K, Novak S, Boccacini AR, Kobe S, The effect of the particle size and the morphology of alumina powders on the processing of green bodies by electrophoretic deposition, *J. Mater. Process. Technol.* **210** (2010) 96–103. <https://doi.org/10.1016/j.jmatprotec.2009.08.007>
130. Kalinina EG, Rusakova DS, Kaigorodov AS, Farlenkov AS, Safronov AP, Formation of Bulk Alumina Ceramics by Electrophoretic Deposition from Nanoparticle Suspensions, *Russ. J. Phys. Chem. A.* **95** (2021) 1519–1528. <https://doi.org/10.1134/S0036024421080148>
131. Kalinina EG, Rusakova DS, Pikalova EYu, Electrophoretic deposition of coatings and bulk compacts using magnesium-doped aluminum oxide nanopowders, *Chim. Techno Acta.* **8** (2021) 20218206, 5072. <https://doi.org/10.15826/chimtech.2021.8.2.06>
132. Hosomi T, Matsuda M, Miyake M, Electrophoretic deposition for fabrication of YSZ electrolyte film on non-conducting porous NiO–YSZ composite substrate for intermediate temperature SOFC, *J. Eur. Ceram. Soc.* **27** (2007) 173–178. <https://doi.org/10.1016/j.jeurceramsoc.2006.04.175>
133. Suzuki HT, Uchikoshi T, Kobayashi K, Suzuki TS, Sugiyama T, Furuya K, Matsuda M, Sakka Y, Munakata F, Fabrication of GDC/LSGM/GDC tri-layers on polypyrrole-coated NiO–YSZ by electrophoretic deposition for anode-supported SOFC, *J. Ceram. Soc. Jpn.* **117** (2009) 1246–1248. <https://doi.org/10.2109/jcersj2.117.1246>
134. Besra L, Compson C, Liu M, Electrophoretic deposition on non-conducting substrates: The case of YSZ film on NiO–YSZ composite substrates for solid oxide fuel cell application, *J. Power Sources.* **173** (2007) 130–136. <https://doi.org/10.1016/j.jpowsour.2007.04.061>
135. E. Kalinina, E. Pikalova, L. Ermakova, N. Bogdanovich, Challenges of Formation of Thin-Film Solid Electrolyte Layers on Non-Conductive Substrates by Electrophoretic Deposition, *Coatings.* **11** (2021) 805. <https://doi.org/10.3390/coatings11070805>
136. Shri Prakash B, Pavitra R, Senthil Kumar S, Aruna ST, Electrolyte bi-layering strategy to improve the performance of an intermediate temperature solid oxide fuel cell: A review, *J. Power Sources.* **381** (2018) 136–155. <https://doi.org/10.1016/j.jpowsour.2018.02.003>
137. Medvedev DA, Pikalova EYu, Development of the Cathode Materials for Intermediate-Temperature SOFCs Based on Proton-Conducting Electrolytes, in: S. Syngellakis, C. Brebbia (Eds.), *Chall. Solut. Russ. Energy Sect.*, Springer International Publishing, Cham, 2018: pp. 173–180. https://doi.org/10.1007/978-3-319-75702-5_20
138. Ishihara T, Shimose K, Kudo T, Nishiguchi H, Akbay T, Takita Y, Preparation of Yttria-Stabilized Zirconia Thin Films on Strontium-Doped LaMnO_3 Cathode Substrates via Electrophoretic Deposition for Solid Oxide Fuel Cells, *J. Am. Ceram. Soc.* **83** (2000) 1921–1927. <https://doi.org/10.1111/j.1151-2916.2000.tb01491.x>
139. Peng Z, Liu M, Preparation of Dense Platinum–Yttria Stabilized Zirconia and Yttria Stabilized Zirconia Films on Porous $\text{La}_{0.9}\text{Sr}_{0.1}\text{MnO}_3$ (LSM) Substrates, *J. Am. Ceram. Soc.* **84** (2004) 283–88. <https://doi.org/10.1111/j.1151-2916.2001.tb00651.x>
140. Basu RN, Altin O, Mayo MJ, Randall CA, Eser S, Pyrolytic Carbon Deposition on Porous Cathode Tubes and Its Use as an Interlayer for Solid Oxide Fuel Cell Zirconia Electrolyte Fabrication, *J. Electrochem. Soc.* **148** (2001) A506. <https://doi.org/10.1149/1.1366620>

141. Kuterbekov KA, Nikonov AV, Bekmyrza KZh, Pavzderin NB, Kabyshev AM, Kubenova MM, Kabdrakhimova GD, Aidarbekov N, Classification of Solid Oxide Fuel Cells, Nanomaterials. **12** (2022) 1059. <https://doi.org/10.3390/nano12071059>
142. Azarian Borojeni I, Raissi B, Maghsoudipour A, Kazemzad M, Talebi T, Fabrication of Solid Oxide Fuel Cells (SOFCs) Electrolytes by Electrophoretic Deposition (EPD) and Optimizing the Process, Key Eng. Mater. **654** (2015) 83–87. <https://doi.org/10.4028/www.scientific.net/KEM.654.83>
143. Talebi T, Haji M, Raissi B, Effect of sintering temperature on the microstructure, roughness and electrochemical impedance of electrophoretically deposited YSZ electrolyte for SOFCs, Int. J. Hydrog. Energy. **35** (2010) 9420–9426. <https://doi.org/10.1016/j.ijhydene.2010.05.079>
144. Matsuda M, Hosomi T, Murata K, Fukui T, Miyake M, Direct EPD of YSZ Electrolyte Film onto Porous NiO-YSZ Composite Substrate for Reduced-Temperature Operating Anode-Supported SOFC, Electrochem. Solid-State Lett. **8** (2005) A8. <https://doi.org/10.1149/1.1828342>
145. Das D, Basu RN, Electrophoretically deposited thin film electrolyte for solid oxide fuel cell, Adv. Appl. Ceram. **113** (2014) 8–13. <https://doi.org/10.1179/1743676113Y.0000000114>
146. Xu Z, Rajaram G, Sankar J, Exploration of Electrophoretic Deposition of YSZ Electrolyte for Solid Oxide Fuel Cells, MRS Proc. **835** (2004) K8.2. <https://doi.org/10.1557/PROC-835-K8.2>
147. Meeppo M, Wattanasiriwech S, Angkavatana P, Wattanasiriwech D, Application of 8YSZ Nanopowder Synthesized by the Modified Solvothermal Process for Anode Supported Solid Oxide Fuel Cells, J. Nanosci. Nanotechnol. **15** (2015) 2570–2574. <https://doi.org/10.1166/jnn.2015.10223>
148. Horri BA, Selomulya C, Wang H, Characteristics of Ni/YSZ ceramic anode prepared using carbon microspheres as a pore former, Int. J. Hydrog. Energy. **37** (2012) 15311–15319. <https://doi.org/10.1016/j.ijhydene.2012.07.108>
149. Horri BA, Selomulya C, Wang H, Electrochemical characteristics and performance of anode-supported SOFCs fabricated using carbon microspheres as a pore-former, Int. J. Hydrog. Energy. **37** (2012) 19045–19054. <https://doi.org/10.1016/j.ijhydene.2012.10.005>
150. Yu SM, Lee KT, Fabrication of YSZ-based Micro Tubular SOFC Single Cell using Electrophoretic Deposition Process, J. Korean Ceram. Soc. **52** (2015) 315–319. <https://doi.org/10.4191/kcers.2015.52.5.315>
151. Ivanov VV, Kotov YuA, Lipilin AS, Safronov AP, Nikonov AV, Kalinina EG, Rempel AIA, Timishenkova OR, Zayats SV, Electrophoretic formation of electrolyte layer on cathode surface of cathode supported SOFC, Altern. Energy Ecol. **66** (2008) 36–50. Available from: <https://naukarus.com/elektroforeticheskoe-formirovanie-tonkoplenochnogo-elektrolita-na-nesuschem-katode-tote>. Access: 19.03.2023
152. Singh M, Zappa D, Comini E, Solid oxide fuel cell: Decade of progress, future perspectives and challenges, Int. J. Hydrog. Energy. **46** (2021) 27643–27674. <https://doi.org/10.1016/j.ijhydene.2021.06.020>
153. Pikalova EY, Kalinina EG, Pikalova NS, Filonova EA, High-Entropy Materials in SOFC Technology: Theoretical Foundations for Their Creation, Features of Synthesis, and Recent Achievements, Materials. **15** (2022) 8783. <https://doi.org/10.3390/ma15248783>
154. Shi H, Su C, Ran R, Cao J, Shao Z, Electrolyte materials for intermediate-temperature solid oxide fuel cells, Prog. Nat. Sci. Mater. Int. **30** (2020) 764–774. <https://doi.org/10.1016/j.pnsc.2020.09.003>
155. Pikalova EYu, Kolchugin AA, Bamburov VG, Ceria-based materials for high-temperature electrochemistry applications, Int. J. Energy Prod. Manag. **1** (2016) 272–283. <https://doi.org/10.2495/EQ-VI-N3-272-283>
156. Kumar CNS, Bauri R, Reddy GS, Phase stability and conductivity of rare earth co-doped nanocrystalline zirconia electrolytes for solid oxide fuel cells, J. Alloys Compd. **833** (2020) 155100. <https://doi.org/10.1016/j.jallcom.2020.155100>
157. Noviyanti AR, Juliandri, Winarsih S, Syarif DG, Malik YT, Septawendar R, Risdiana, Highly enhanced electrical properties of lanthanum-silicate-oxide-based SOFC electrolytes with co-doped tin and bismuth in $\text{La}_{9.33-x}\text{Bi}_x\text{Si}_{6-y}\text{Sn}_y\text{O}_{26}$, RSC Adv. **11** (2021) 38589–38595. <https://doi.org/10.1039/D1RA07223D>
158. Cheng M-Y, Shiau C-Y, Lin P-H, Chang J-C, Anode-supported solid oxide fuel cell with electrophoretic deposition-derived electrolyte operated under single-chamber conditions and a methane–air mixture, J. Solid State Electrochem. **15** (2011) 773–779. <https://doi.org/10.1007/s10008-010-1153-2>
159. Kalinina EG, Pikalova EYu, Formation of a Single- and Two-Layer Solid Electrolyte by Electrophoresis on Anodic Substrates Metalized with Silver or Platinum, Russ. J. Phys. Chem. A. **96** (2022) 2763–2773. <https://doi.org/10.1134/S0036024422120147>
160. Kalinina EG, Rusakova DS, Shubin KS, Ermakova LV, Pikalova EYu, CeO₂-based thin-film electrolyte membranes for intermediate temperature SOFCs: Direct electrophoretic deposition on the supporting anode from additive-modified suspensions, Int. J. Hydrog. Energy. (2023) In Press. <https://doi.org/10.1016/j.ijhydene.2023.01.159>
161. Trulsson M, Jönsson B, Labbez C, On the origin of the halo stabilization, Phys. Chem. Chem. Phys. **15** (2013) 541–545. <https://doi.org/10.1039/C2CP42404E>
162. Tohver V, Smay JE, Braem A, Braun PV, Lewis JA, Nanoparticle halos: A new colloid stabilization mechanism, Proc. Natl. Acad. Sci. **98** (2001) 8950–8954. <https://doi.org/10.1073/pnas.151063098>
163. Hu S, Finklea H, Li W, Li W, Qi H, Zhang N, Liu X, Alternating Current Electrophoretic Deposition of Gadolinium Doped Ceria onto Yttrium Stabilized Zirconia: A Study of the Mechanism, ACS Appl. Mater. Interfaces. **12** (2020) 11126–11134. <https://doi.org/10.1021/acsami.9b17504>
164. Yamaji K, Performance of anode-supported SOFCs fabricated with EPD techniques, Solid State Ion. **175** (2004) 165–169. <https://doi.org/10.1016/j.ssi.2004.09.032>
165. Mathews T, Fabrication of $\text{La}_{1-x}\text{Sr}_x\text{Ga}_{1-y}\text{Mg}_y\text{O}_{3-(x+y)/2}$ thin films by electrophoretic deposition and its conductivity measurement, Solid State Ion. **128** (2000) 111–115. [https://doi.org/10.1016/S0167-2738\(99\)00308-2](https://doi.org/10.1016/S0167-2738(99)00308-2)
166. Bozza F, Polini R, Traversa E, Electrophoretic Deposition of Dense Sr- and Mg-Doped LaGaO₃ Electrolyte Films on Porous La-Doped Ceria for Intermediate Temperature Solid Oxide Fuel Cells, Fuel Cells. **8** (2008) 344–350. <https://doi.org/10.1002/face.200800022>

167. Medvedev D, Murashkina A, Pikalova E, Demin A, Podias A, Tsiakaras P, BaCeO₃: Materials development, properties and application, *Prog. Mater. Sci.* **60** (2014) 72–129. <https://doi.org/10.1016/j.pmatsci.2013.08.001>
168. Haile SM, Staneff G, Ryu KH, Non-stoichiometry, grain boundary transport and chemical stability of proton conducting perovskites, *J. Mater. Sci.* **36** (2001) 1149–1160. <https://doi.org/10.1023/A:1004877708871>
169. Mercadelli E, Montaleone D, Gondolini A, Pinasco P, Sanson A, Tape-cast asymmetric membranes for hydrogen separation, *Ceram. Int.* **43** (2017) 8010–8017. <https://doi.org/10.1016/j.ceramint.2017.03.099>
170. Ding Y, Li Y, Huang W, The role of Ba concentration on the structural characteristics and electrical conductivities of Ba_xCe_{0.9Y_{0.1}O_{3-α}}, *Mater. Res. Bull.* **95** (2017) 328–333. <https://doi.org/10.1016/j.materresbull.2017.08.004>
171. Pikalova E, Medvedev D, Effect of anode gas mixture humidification on the electrochemical performance of the BaCeO₃-based protonic ceramic fuel cell, *Int. J. Hydrog. Energy.* **41** (2016) 4016–4025. <https://doi.org/10.1016/j.ijhydene.2015.11.092>
172. Kalinina EG, Pikalova EYu, Farlenkov AS, Electrophoretic Deposition of Thin-Film Coatings of Solid Electrolyte Based on Microsize BaCeO₃ Powders, *Russ. J. Appl. Chem.* **91** (2018) 934–941. <https://doi.org/10.1134/S1070427218060095>
173. Pikalova EYu, Kolchugin AA, The Influence of the Substituting Element (M = Ca, Sr, Ba) in La_{1.7}M_{0.3}NiO_{4+δ} on the Electrochemical Performance of the Composite Electrodes, *Eurasian Chem.-Technol. J.* **18** (2016) 3. <https://doi.org/10.18321/ectj386>
174. Tarutin AP, Danilov NA, Kalinin AA, Murashkina AA, Medvedev DA, Ba-doped Pr₂NiO_{4+δ} electrodes for proton-conducting electrochemical cells. Part I: Structure, mechanical, and chemical properties, *Int. J. Hydrog. Energy.* (2022) In Press. <https://doi.org/10.1016/j.ijhydene.2022.11.175>
175. Tarutin AP, Gorshkov MYu, Bainov IN, Vdovin GK, Vylkov AI, Lyagaeva JG, Medvedev DA, Barium-doped nickelates Nd_{2-x}Ba_xNiO_{4+δ} as promising electrode materials for protonic ceramic electrochemical cells, *Ceram. Int.* **46** (2020) 24355–24364. <https://doi.org/10.1016/j.ceramint.2020.06.217>
176. Zunic M, Chevallier L, Di Bartolomeo E, D'Epifanio A, Licocchia S, Traversa E, Anode Supported Protonic Solid Oxide Fuel Cells Fabricated Using Electrophoretic Deposition, *Fuel Cells.* **11** (2011) 165–171. <https://doi.org/10.1002/fuce.200900104>
177. Zunic M, Chevallier L, Deganello F, D'Epifanio A, Licocchia S, Di Bartolomeo E, Traversa E, Electrophoretic deposition of dense BaCe_{0.9}Y_{0.1}O_{3-x} electrolyte thick-films on Ni-based anodes for intermediate temperature solid oxide fuel cells, *J. Power Sources.* **190** (2009) 417–422. <https://doi.org/10.1016/j.jpowsour.2009.01.046>
178. Medvedev D, Lyagaeva J, Plaksin S, Demin A, Tsiakaras P, Sulfur and carbon tolerance of BaCeO₃-BaZrO₃ proton-conducting materials, *J. Power Sources.* **273** (2015) 716–723. <https://doi.org/10.1016/j.jpowsour.2014.09.116>
179. Bozza F, Bonanos N, Fabrication of supported Ca-doped lanthanum niobate electrolyte layer and NiO containing anode functional layer by electrophoretic deposition, *Solid State Ion.* **213** (2012) 98–102. <https://doi.org/10.1016/j.ssi.2011.05.017>
180. Sun W, Jiang Y, Wang Y, Fang S, Zhu Z, Liu W, A novel electronic current-blocked stable mixed ionic conductor for solid oxide fuel cells, *J. Power Sources.* **196** (2011) 62–68. <https://doi.org/10.1016/j.jpowsour.2010.07.038>
181. Kalinina EG, Pikalova EYu, Electrophoretic deposition of dense anode barrier layers of doped ZrO₂ and BaCeO₃ on a supporting Ce_{0.8}Sm_{0.2}O_{2-δ} solid electrolyte: Problems and search for solutions in SOFC technology, *Int. J. Hydrog. Energy.* (2023) In press. <https://doi.org/10.1016/j.ijhydene.2023.02.042>